

# Fatigue Crack growth study of composite patch repaired Aluminum Al 2014-T6 panel under Variable Amplitude Loading

Sammed Pandharkar

A Thesis Submitted to  
Indian Institute of Technology Hyderabad  
In Partial Fulfillment of the Requirements for  
The Degree of Master of Technology



Department of Mechanical and Aerospace Engineering

June 2015

## Declaration

I declare that this written submission represents my ideas in my own words, and where ideas or words of others have been included, I have adequately cited and referenced the original sources. I also declare that I have adhered to all principles of academic honesty and integrity and have not misrepresented or fabricated or falsified any idea/data/fact/source in my submission. I understand that any violation of the above will be a cause for disciplinary action by the Institute and can also evoke penal action from the sources that have thus not been properly cited, or from whom proper permission has not been taken when needed.

Pandharkar

(Signature)

Sammed Pandharkar

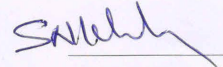
(Sammed Pandharkar)

ME10B14M000005

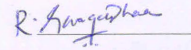
(Roll No.)

## Approval Sheet

This Thesis entitled Fatigue Crack growth study of composite patch repaired Aluminum Al 2014-T6 panel under Variable Amplitude Loading by Sammed Pandharkar is approved for the degree of Master of Technology from IIT Hyderabad



(Dr. Syed Nizamuddin Khaderi) Examiner  
Assistant Professor  
Department of Mechanical and Aerospace Engineering  
Indian Institute of Technology Hyderabad



(Dr. Gangadharan Raju) Examiner  
Assistant Professor  
Department of Mechanical and Aerospace Engineering  
Indian Institute of Technology Hyderabad



(Dr. Ramji M) Adviser  
Associate Professor  
Department of Mechanical and Aerospace Engineering  
Indian Institute of Technology Hyderabad



(Dr. S. Suriya Prakash) Chairman  
Assistant Professor  
Department of Civil Engineering  
Indian Institute of Technology Hyderabad

## Acknowledgements

First of all, I am grateful to god for the health, well-being and opportunity.

I wish to express my sincere thanks to Department of Mechanical and Aerospace Engineering, IIT Hyderabad, for providing me with all the necessary facilities for the research.

I express my sincere gratitude towards my project advisor Dr. M. Ramji, for the continuous encouragement and valuable guidance.

I take this opportunity to express gratitude to all of the Department faculty members for their help and support. I also thank my parents for the unceasing encouragement, support and attention. I am also grateful to my partner who supported me through this venture.

I express my sincere gratitude towards Optics lab members, Central workshop, and all of my friends, who were always there for any help.

I also place on record, my sense of gratitude to one and all, who directly or indirectly, have lent their hand in this venture.

# Dedication

Dedicated to parents, friends and teachers

## Abstract

In this modern era, use of aircrafts in freight, public transport and warfare is increasing day by day. With this increasing demand and ever limited supply, the need of efficient use of already available resources is high. This leads to a need of increasing the lifespan of an aircraft, so it can provide service for longer period of time and ultimately give a relief to from financial stress of replacing the aging aircraft with a new one.

The aircraft in its whole lifespan goes through many kinds of damages which include general fatigue damage from numerous take-off, inflight, landing, taxiing and ground handling cycles, degradation occurring due to environmental damages, air turbulence, bird strikes etc. to name a few. These damages severely degrade the lifespan of the aircraft. The need of increasing the lifespan calls for damage repair methodologies to be applied. Among these, adhesively bonded composite patch repair technique is mostly preferred. There is lot of research work carried out in this area concerning constant amplitude fatigue life estimation of composite patch repaired metallic panels made of Aluminium alloy. But very less research work exists in the area of fatigue crack growth study of composite patch repaired component under spectrum load.

In this work, numerical prediction of the fatigue life of Al 2014-T6 panel with a straight center crack followed by an inclined center crack repaired by single- and double-sided adhesively bonded Carbon fiber reinforced polymer (CFRP) patch under FALSTAFF variable amplitude loading is carried out. A 3D finite element analysis (FEA) based study is done using Zencrack 7.6 and ANSYS 12.1 to model the fatigue crack growth in both unrepaired and repaired panel. The adhesive layer between the panel and patch is modelled using bilinear cohesive law involving contact elements. In case of single-sided repaired panel, a non-uniform crack growth through its thickness is observed. Further, it is showed that the fatigue life of the double-sided repaired panel is twice that of the single-sided repaired panel.

# Contents

Acknowledgements . . . . .	iii
Abstract . . . . .	vi
<b>Nomenclature</b>	<b>viii</b>
<b>1 Introduction and Literature Review</b>	<b>4</b>
1.1 Repair technology: An overview . . . . .	4
1.2 Motivation . . . . .	5
1.3 Literature review . . . . .	6
1.4 Scope and Objective . . . . .	7
1.5 Thesis layout . . . . .	7
<b>2 Fatigue Crack growth analysis under variable amplitude loading using Finite Element Method</b>	<b>8</b>
2.1 Introduction . . . . .	8
2.2 Geometry and Material Properties . . . . .	10
2.2.1 Geometry . . . . .	10
2.2.2 Material Properties . . . . .	11
2.3 Variable Amplitude Loading . . . . .	12
2.3.1 Introduction . . . . .	12
2.3.2 FALSTAFF Loading . . . . .	13
2.4 Fatigue crack growth modelling using FEA . . . . .	15
2.4.1 FEA Model Description . . . . .	16
2.4.2 Patch Modelling- CZM . . . . .	18
2.4.3 Introduction to Zencrack . . . . .	18
2.4.4 Working of Zencrack . . . . .	19
2.5 Results and Discussion . . . . .	23
2.5.1 Fatigue life prediction . . . . .	23
2.5.2 SIF Variation . . . . .	23
2.5.3 Crack front shapes . . . . .	25
2.6 Closure . . . . .	26
<b>3 Experimental Investigation of Fatigue crack growth</b>	<b>27</b>
3.1 Specimen fabrication . . . . .	27
3.2 Experimental Setup . . . . .	29

3.3	Post-processing . . . . .	30
3.4	Results and discussion . . . . .	31
3.5	Closure . . . . .	33
<b>4</b>	<b>Conclusions and Recommendations</b>	<b>34</b>
4.1	Conclusions . . . . .	34
4.2	Recommendations for future work . . . . .	35
<b>A</b>	<b>Matlab Code to edit the FALSTAFF variable amplitude loading</b>	<b>36</b>
<b>B</b>	<b>Writing Zencrack Macro File</b>	<b>38</b>
<b>C</b>	<b>Ansys 12.1 APDL codes</b>	<b>41</b>
C.1	APDL code for unrepaired panel . . . . .	41
C.2	APDL code for single sided repaired panel . . . . .	46
C.3	APDL code for double sided repaired panel . . . . .	61
	<b>References</b>	<b>82</b>



# List of Figures

1.1	F-89 Scorpion crash. Aug. 30 1952 [1] . . . . .	4
1.2	BOAC Flight 781 Crash pictures (a):DH Comet 1 BOAC Heathrow 1953, before take-off [2]; (b):recovered wreckage assembled digitally depicting fracture initialization point [3]; (c): Picture of wrecked fuselage [4] . . . . .	5
2.1	Full-Scale Fatigue Testing of the F/A-18 Fighter Aircraft [5] . . . . .	8
2.2	Geometry of basic models that are used in FEA. (a): Straight Center Cracked Specimen; (b): Center Slant Cracked Specimen . . . . .	10
2.3	Sketch of the patch geometry taken from ref. [6] . . . . .	11
2.4	Constant amplitude fatigue loading [7] . . . . .	13
2.5	Variable amplitude fatigue loading: Block loading [8] . . . . .	13
2.6	Variable amplitude fatigue loading: Spectrum loading [9] . . . . .	14
2.7	Genesis program user interface [10] . . . . .	14
2.8	FALSTAFF Loading sequence . . . . .	15
2.9	Modified FALSTAFF Loading sequence . . . . .	15
2.10	Finite element model of SCC and CSC specimens with out any crack tip elements (a) straight center crack (b) center slant crack . . . . .	16
2.11	Zoomed in view of uncracked finite element model. (a)SCC specimen and (b) CSC specimen. Red lines designate the intended crack length which is going to be modelled by Zencrack 7.6 . . . . .	17
2.12	FEA model of composite patch . . . . .	19
2.13	Working of Zencrack 7.6 [11] . . . . .	20
2.14	Crack block s02t19x1 . . . . .	21
2.15	Mesh after crack block is inserted by Zencrack 7.6 software . . . . .	22
2.16	The local coordinate system is generated to measure crack opening displacements [11] . . . . .	22
2.17	Crack length v/s number of modified FALSTAFF blocks for the SCC specimen obtained using FEA . . . . .	24
2.18	Crack length v/s number of modified FALSTAFF blocks for the CSC specimen obtained using FEA . . . . .	24
2.19	SIF variation for SCC panel. a: $K_I$ variation; b: $K_{II}$ variation . . . . .	25
2.20	SIF variation for CSC panel. a: $K_I$ variation; b: $K_{II}$ variation . . . . .	25
2.21	Crack front shapes and number of cycles corresponding to similar crack growth . . . . .	26
3.1	Line diagrams of the specimens: a) SCC specimen, b) CSC specimen . . . . .	28

3.2	Zoomed view of specimen showing the speckle pattern . . . . .	29
3.3	Experimental setup . . . . .	30
3.4	Examples of grabbed images a) from the back of the specimen, b) from the front of the specimen . . . . .	31
3.5	crack length versus Number of cycles plot . . . . .	31
3.6	Shape of the crack front after failure of the specimen. a) A microscopic image; b) a macroscopic image . . . . .	32
3.7	$K_I$ versus crack length plot for experiment. It is also compared with FEA result. . .	32
A.1	. . . . .	37
B.1	. . . . .	39
B.2	. . . . .	39
B.3	. . . . .	40

# List of Tables

2.1	Aluminium Al 2014-T6 alloy composition [12] . . . . .	11
2.2	Material properties of Aluminium Al 2014-T6 specimen . . . . .	12
2.3	Material properties of Araldite 2011 adhesive and CFRP laminate [13, 14] . . . . .	12
2.4	Paris' Law Constants [15] . . . . .	12
2.5	Adhesive material properties . . . . .	18

# Chapter 1

## Introduction and Literature Review

### 1.1 Repair technology: An overview

Any aircraft in its entire service life goes through numerous flight cycles. During thousands of hours of service life, the structure of aircraft gets affected by many kinds of damages. It includes incidental damages such as air turbulence, bird strike etc., and also continually occurring damages such as environmental corrosion and fatigue damages. Fatigue load acting on aircraft structure under actual service condition is usually the main threat to an aircraft's life span. A flight cycle includes ground handling of an aircraft, taxiing on the runway, take-off, in-flight hours, and finally landing. During this cycle, aircraft structure experiences many repetitive loads. During ground handling, the fuselage of aircraft bears the weight of the wings and in air, the roles are reversed i.e. wings take the load of fuselage. This explains the reversing load that is being applied on the fuselage and wing joint. The main structure also bears varying degree of fatigue load during a flight cycle. Fatigue load leads to growth of micro-cracks in aircraft structure, also it helps grow the cracks which are already present in the structure due to other reasons.

In the first case study, an Air Force F-89 Scorpion tore itself apart above 51,000 spectators at Detroit, MI Air Show on Aug 30 1952 and carried its pilot, a Korean jet ace, and his radar observer to their deaths at the International Aviation Exposition [16]. Fig. 1.1 shows the accident.



Figure 1.1: F-89 Scorpion crash. Aug. 30 1952 [1]

In the second case study, British Overseas Airways Corporation Flight 781, a de Havilland DH.106

Comet 1, registered G-ALYP,[1] took off from Ciampino Airport in Rome, Italy, en route to Heathrow Airport in London, England. At about 10:51 GMT on January 10, 1954, the aircraft suffered an explosive decompression at altitude and crashed into the Mediterranean Sea, killing everyone on board. The cause of the crash has been found as improper inspection of incidental damage to structure, causing a fracture to go un-noticed. Investigators found that fractures started in the roof of the cabin, a window then smashed into the elevators, the rear fuselage then tore away, the outer wing structure fell, then the outer wing tips and finally the cockpit broke away and fuel from the wings set the debris on fire [17]. Fig. 1.2 shows picture of the plane before take-off, digital assembly of wreckage and picture of wreckage.

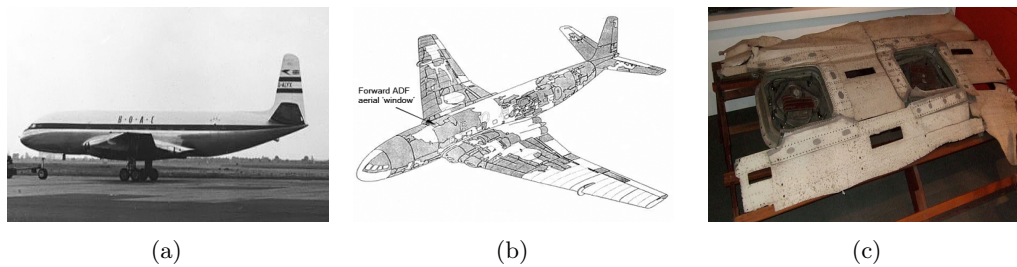


Figure 1.2: BOAC Flight 781 Crash pictures (a):DH Comet 1 BOAC Heathrow 1953, before take-off [2]; (b):recovered wreckage assembled digitally depicting fracture initialization point [3]; (c): Picture of wrecked fuselage [4]

The examples we discussed are majorly happened because of structural failure. Structural failures are nothing but the small cracks that are grown overtime. These cracks are bound to occur during service life of the aircraft. Therefore, repair or replacement of the parts while damages are benign is a must. Generally the approximate cost of replacement of parts are extremely costly especially in modern military aircrafts. But the limited budget and industrial demands, the need for repair is high to enable us to use the aircraft for longer periods of time.

Generally, the repair is done by either drilling holes in front of cracks, repairs with mechanical fasteners e.g. bolts, rivets etc., or adhesively bonded patch repairs. Drilling holes in front of the crack front reduces the crack propagation rate significantly, as crack has to start from a new location when the crack front reaches the hole. But the structural integrity decreases due to the drilling operations. Repairs with mechanical fasteners also includes drilling holes for bolts which decreases the load carrying capacity. Also, there are high stress concentration zones present near bolt contact zone. Baker [18] carried out experimental fatigue investigation on cracked panel with both bolted repair and boron/epoxy composite patch repair under fatigue loading. In that, he discovered that fatigue life improvement of composite patch repair was twice that of bolted repair. Apart from that, composite patches have higher strength to weight ratio as compared to mechanical fasteners. All of these factors are the reason why composite patch repairs are being increasingly used in this modern age.

## 1.2 Motivation

Currently , fatigue crack growth analysis of cracked panel have been done on very limited set of parameters. One can find research work on fatigue crack growth analysis of straight center cracked

with composite patch repair under constant amplitude loading. But those studies do not take the fact into consideration that most of the cracks in real situation are mixed mode. And the loading in real life application are always variable amplitude loading in contrary to widely studied constant amplitude loading cases. Therefore, there is a need to study the fatigue life of CFRP repaired aluminium AL 2014-T6 panel with straight center crack as well as inclined center crack individually. This can be done in two ways, numerical study involving FEA and experimental analysis. These two methods can be done together validating the results both qualitatively and quantitatively.

### 1.3 Literature review

Repairing accumulated fatigue cracks in aircraft structure using composite patch repairs have many advantages over conventional mechanical fastening or riveting such as reduced stress concentration, efficient load transfer, improved fatigue behavior, restored stiffness and strength, reduced corrosion and handling of complex patch configuration. Typically, there are two types of patch work that are prevalent in composite repair: single-sided (un-symmetrical patch) and double-sided (symmetrical patch) repair. Double sided repair provides higher SIF reduction but single sided is generally more viable way of repair in practice.

During past half century, many researchers have examined the behaviour of crack propagation under Variable Amplitude fatigue loads. In 1979, Schijve [19] had defined and classified various types of Variable amplitude Loadings. He also gave an insight on crack closure effect in Variable amplitude loadings (VAL). Sunder (1979) [20] proposed mathematical model of fatigue crack propagation under VAL. He also studied application of the model to overload situations. In 1985, Schijve, along with A M Vlutters and J C Provo Klutt studied crack growth in aluminium alloy 2024-T3 under flight simulation loads miniTWIST and short FALSTAFF loadings [21]. In which, fatigue life of center cracked, CT plate with hole specimen were estimated and compared to respectively corresponding full size load spectrums TWIST and FALSTAFF. Sunder [22] in 1985 proposed algorithms for computer controlled crack propagation tastings under random load. It was used to predict Fatigue crack propagation under spectrum loading on thin walled aircraft structures [23]. In 1997, Newman, Jr. [24] predicted crack growth under VAL in thin-sheet AL2024-T3 alloys using plasticity induced crack closure model. In 2007 [25], Manjunatha studied the prediction of optimum spectrum for full scale fatigue load. In which he tried to reduce total number of reversals in FALSTAFF loading and compared with experimental results. In 2013, [26] he studied fatigue behaviour of glass fiber reinforced hybrid particles modified epoxy nanocomposite under WISPERX spectrum.

After studying the mechanics of both the single- and double-sided repair of an inclined center cracked panel using FEA, Ramji and Srilakshmi have concluded that behavior of single side patch repaired panel is very different from double-sided patch repaired one [15]. Further, Ramji et al. [6] have investigated the influence of different patch shapes on the performance of a double-sided patch repair panel. They found that the extended octagonal patch shape performed better in case of SIF reduction. Recently, Hosseini-Toudeshky et al. [27] implemented the progressive failure analysis of a repaired panel using the cohesive zone modeling at patch/panel interface . Maligno et, al. [28] carried out experimental and FEA analysis of fatigue crack growth of cracked panel with composite patch repair. They have modelled the debonding by degrading the material property of the adhesive element at the interface and predicted the fatigue life.

## 1.4 Scope and Objective

Based upon the introduction to aircraft failures and literature study, behaviour of cracked panel with composite patch repair under constant amplitude loading are studied extensively, but there is a need to study the same under variable amplitude loading. The following are the objectives of this study:

- To study fatigue behaviour of Al 2014-T6 specimen with straight center crack (SCC) and center slant crack (CSC) under FALSTAFF variable amplitude loading using FEA.
- To estimate the fatigue life improvement by repairing the panels on single side with CFRP patch.
- To estimate the fatigue life improvement by repairing the panels on both sides with CFRP patch.
- To find a method to test the specimens experimentally under variable amplitude loading.
- To compare the experimental results to FEA thus validating the numerical analysis.

## 1.5 Thesis layout

This section discusses the layout of the whole thesis. Chapter 1 contains introduction, literature review, motivation and objective of the thesis work. Chapter 2 covers the finite element study of composite repaired straight center and center slant cracked panel under variable amplitude fatigue loading. It includes the description of loading and methodology used to execute the numerical analysis. Chapter 3 contains the method used to conduct experimental fatigue crack growth analysis of the panel and results comparison with results got in FEA. Chapter 4 contains conclusions of the thesis work and future recommendation. Appendix A contains the MATLAB code that was used to edit the FALSTAFF loading to eliminate the control points in compressive zone. Appendix B contains the methodology of creating the Zencrack macro file which is used to run the FE simulation. Appendix C contains the Ansys 12.1 APDL codes which were used in numerical study.

## Chapter 2

# Fatigue Crack growth analysis under variable amplitude loading using Finite Element Method

### 2.1 Introduction

Finite element method is a numerical method for solving a differential or integral equation. Finite Element Analysis (FEA) is now widely used for prediction for structural load distribution, deformation speculation ,damage prediction etc. As we have already discussed, testing aircraft structure under fatigue loading and predicting the damage initialization and its growth is extremely important in regards to speculate the remaining service life of a structure. Hypothetically, this can always be done through full scale fatigue tests. But in real world, there are very few such testing facilities available [29, 5], and the time and cost required to conduct such large scale tests are not always available. Figure 2.1 depicts a full scale fatigue testing of F/A-18 aircraft.



Figure 2.1: Full-Scale Fatigue Testing of the F/A-18 Fighter Aircraft [5]

To overcome these limitations, widely accepted solution is to model the problem in Finite Element and verify the model through small scale fatigue coupon tests. Current study focuses upon fatigue crack growth (FCG) analysis of a Aluminium Al 2014-T6 panel with straight center crack (SCC specimen) and with Center slant crack (CSC specimen) under unrepaired, single sided repaired



and double sided repaired conditions. Fatigue life prediction of a cracked specimen with composite patch repair is complicated because of factors such as possible in failure modes like patch debonding, crack growth in aluminium panel and combination of both. In past, Ouinas et al. [30] have studied the crack growth behaviour of an aluminium plate cracked at the tip and repaired with a bonded boron/epoxy composite patch. Ouinas et al. [31] also have studied the SIF of repaired cracks through numerical analysis. Papanikos et al. [32, 33] have studied the progressive damage modelling of bonded composite repairs. In it, they have established that stress concentration is a function of patch thickness and adhesive thickness. Also, initialization of patch debonding is dependent on patch geometrical factors such as patch thickness, adhesive thickness, patch length, tapered length. Aforementioned studies are based upon debonding behaviour under static load. Dae-Cheol and Jung-Ju [34] studied FCG behaviour of cracked aluminium Al 7075-T6 thick plate repaired with adhesively bonded graphite/epoxy composite patch. In 2013, Maligno et al. [28] numerically studied FCG behaviour of thick crack aluminium Al 7075-T6 alloy plate repaired with bonded graphite/epoxy composite patch. The authors had used Zencrack software for FCG analysis. In 2013, Hossein Hosseini-Toudeshky et al. [27] studied FE based failure analysis of initiation and propagation of debonding in the adhesive layer when it occurs concurrently with the growth of an initial crack in a single-side repaired aluminium panels by composite patches under cyclic loading. They have implemented Cohesive zone modelling concept using interface element for modelling of adhesive layer.

Most of the existing work is based upon fatigue crack growth study of patched metal panels and is limited to constant amplitude fatigue loading. For variable amplitude loading situations, Sunder [20] proposed a mathematical model of fatigue crack growth under VAL. He has used crack closure concept to develop the model and describes both acceleration and retardation behaviour of crack growth, also delayed retardation after overloads. In 2011, Ziegler et al. [35] studied application of strip-yield model to predict crack growth under variable amplitude fatigue loading on Middle crack tension specimen. Moreno et al. [36] have used NASGRO software to study fatigue crack growth under variable amplitude loading in Aluminium alloy AL 2024-T351 alloy. They have also compared the results with experimental data.

In the present chapter, geometry and material properties of the specimen under study is explained, which contains both Straight Center Crack (SCC) specimen and Center slant Crack (CSC) specimen in unrepaired, single sided repaired and double sided repaired specimens. The study is based upon FALSTAFF variable amplitude loading which is explained in next section. Finite element modelling of the specimen and patch with adhesive modelling is explained later followed by the Zencrack 7.6 software which is used to perform FCG analysis is explained. Finally, results obtained from the analysis are discussed.

## 2.2 Geometry and Material Properties

This section describes the geometry of the FEA model and enlists the material properties which are going to be useful in the analysis.

### 2.2.1 Geometry

In FEA, the model which is going to be analysed is depicted in Figure 2.2. The dimensions are 40 mm  $\times$  160 mm  $\times$  3 mm. In SCC specimen, the crack length is of  $2a = 10$  mm length. In CSC specimen, the crack is inclined at  $\beta = 45^\circ$  angle, but also is of  $2a = 10$  mm length. The thickness is 3 mm and corresponds to plain stress condition (thick plate).

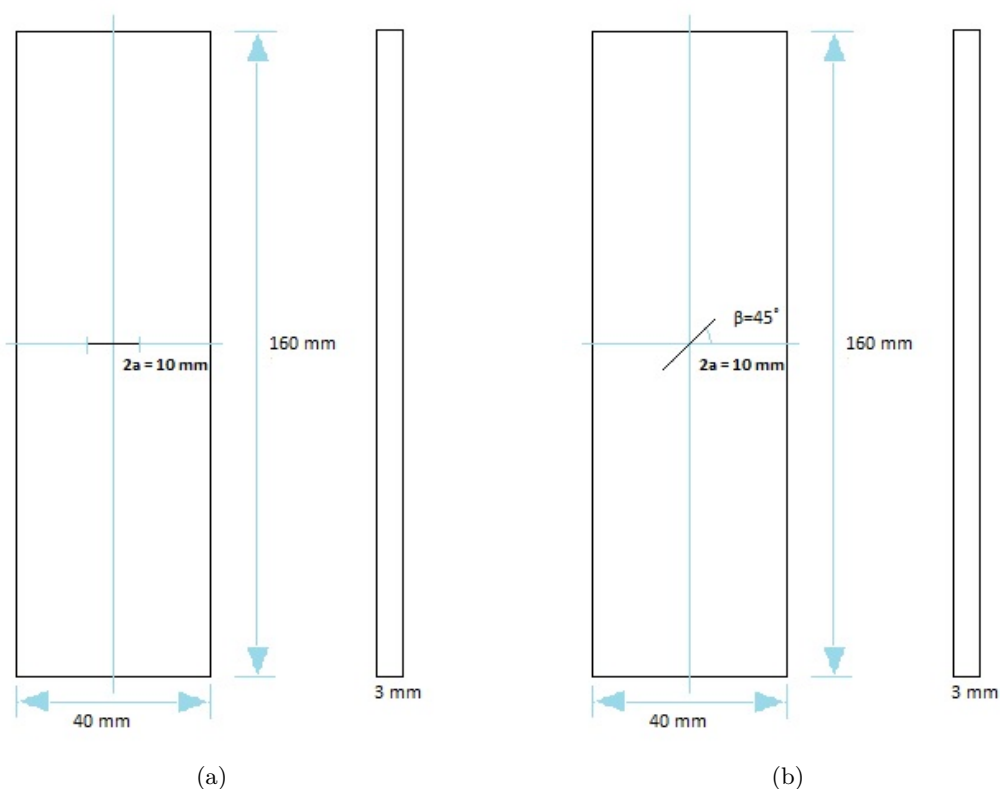


Figure 2.2: Geometry of basic models that are used in FEA. (a): Straight Center Cracked Specimen; (b): Center Slant Cracked Specimen

The patch geometry is depicted in Figure 2.3. The optimum patch shape is obtained through parametric optimization study carried out by Ramji et al. [37]. The patch thickness corresponds to 6 layers of  $[0^\circ]$  CFRP Laminates and the dimensions are taken from ref. [6].

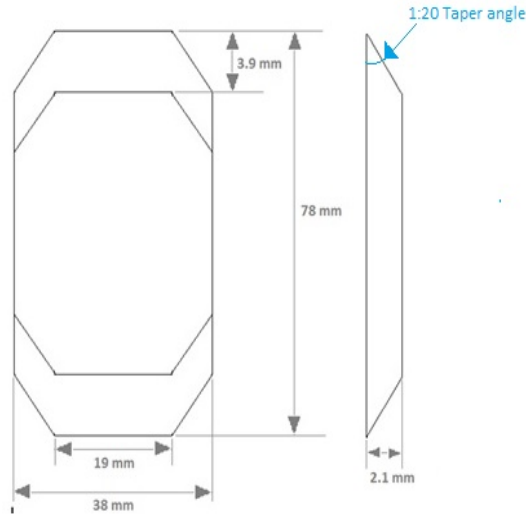


Figure 2.3: Sketch of the patch geometry taken from ref. [6]

### 2.2.2 Material Properties

Current study uses Aluminium Al 2014-T6 alloy as the cracked specimen material. It is widely used in bicycle industry. It is easily machined in certain tempers, and one of the strongest available aluminium alloys, as well as having a higher hardness. However, it is difficult to weld, as it may develop cracking after the process.

The composition of the alloy is given in Table 2.1 taken from ref. [12]

Table 2.1: Aluminium Al 2014-T6 alloy composition [12]

Component	Wt. %
Al	90.4 - 95 (Calculated as remainder)
Cr	Max 0.1
Cu	3.9 - 5
Fe	Max 0.7
Mg	0.2 - 0.8
Mn	0.4 - 1.2
Other, each	Max 0.05
Other, total	Max 0.15
Si	0.5 - 1.2
Ti	Max 0.15
Zn	Max 0.25

Material properties of the specimen are to be fed in FEA package as input before running the simulation to ensure correlation with experimental results. The required properties for the simulation are evaluated experimentally using Digital Image Correlation by Srilakshmi and Ramji [38]. They have used ASTM E-08 standard. The properties that are obtained and used in simulation as shown below in Table 2.2

Table 2.2: Material properties of Aluminium Al 2014-T6 specimen

Material Property	Value
Young's Modulus, $E$	73.1 GPa
Poisson's ratio, $\nu$	0.33

In case of single sided and double sided repaired panel, unidirectional CFRP laminate with  $0^\circ$  lay up has been used as the repair patch material. The material properties of the composite as well as the adhesive, in this case Araldite 2011 adhesive, needs to be determined. Table 2.3 contains the properties of the adhesive and CFRP which are take from [13, 14].

Table 2.3: Material properties of Araldite 2011 adhesive and CFRP laminate [13, 14]

Material	$E_x$ (GPa)	$E_y, E_z$ (GPa)	$\nu_{xy}, \nu_{xz}$	$\nu_{yz}$	$G_{xy}, G_{xz}$ (GPa)	$G_{yz}$ (GPa)
Adhesive	1.148	-	0.4	-	-	-
CFRP (Carbon/epoxy)	81.9	6.15	0.34	0.5	2.77	2.05

In this study, the fatigue crack growth simulation is based on Paris' law. More is explained in 2.4.4. The basic Paris' law is formulated in Eqn. 2.1 as given below.

$$\frac{da}{dN} = C\Delta K^m \quad (2.1)$$

For the simulation, one needs to know the Paris' law constants  $C$  and  $m$ . Srilakshmi et al. [15] have determined these constants for Al 2014-T6 experimentally by doing baseline fatigue crack growth tests suggested in ASTM E-647 standard [39]. The values are tabulated in Table 2.4.

Table 2.4: Paris' Law Constants [15]

Constant	Value
$C$	5.21e-11
$m$	3.28

## 2.3 Variable Amplitude Loading

### 2.3.1 Introduction

Fatigue loading can be broadly classified into two categories: constant amplitude fatigue loading and variable amplitude fatigue loading. Constant amplitude fatigue loading, as name suggests, has a constant amplitude until final fracture. The mean load also remains fixed. Therefore, it can be described by mean load and amplitude.

In Variable amplitude, there are two major categories: 1) Block loading, 2) Spectrum loading. In block loading, the load sequence is a collection of two or more 'blocks' of constant amplitude loading sequence, which are repeated one after another. The parameters required to define block loading is

number of blocks in a sequence, number of cycles in each block and the mean load and amplitude of each block. In spectrum loading, the loading can only be defined by 'reversal points' i.e. load levels from which the loading reverses the direction. Spectrum loadings are in general experimentally recorded and used in simulations/experiments as real life load sequence. Figures 2.4, 2.5 and 2.6 depict the aforementioned fatigue loadings respectively.

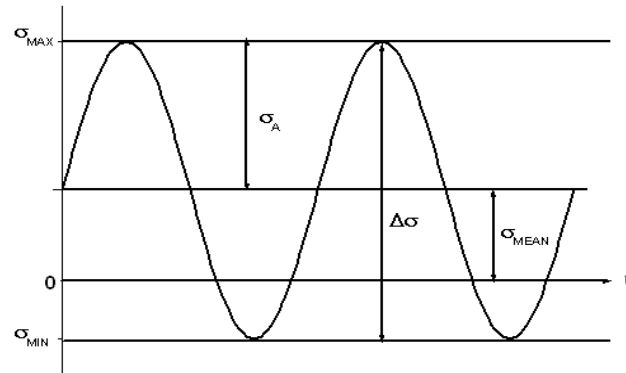


Figure 2.4: Constant amplitude fatigue loading [7]

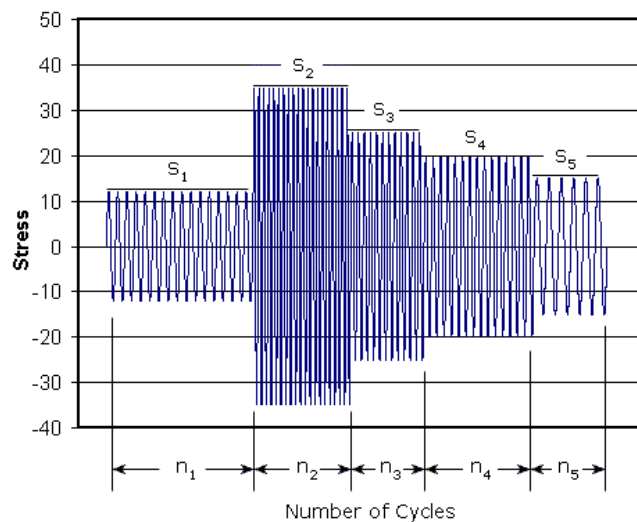


Figure 2.5: Variable amplitude fatigue loading: Block loading [8]

The current study is based upon the crack growth behaviour under variable amplitude spectrum loading. Next section describes the loading which this study uses in detail.

### 2.3.2 FALSTAFF Loading

The fatigue life estimation by FEM simulation or by experiment can be further enriched if the load spectrum which is used is representative of stresses actually experienced by the structure in service. The distribution and number of stress cycles, and the order in which the loads are applied define the stress spectrum loading. Service load spectra can be estimated by monitoring the strains at critical regions of the component operating under typical service conditions.

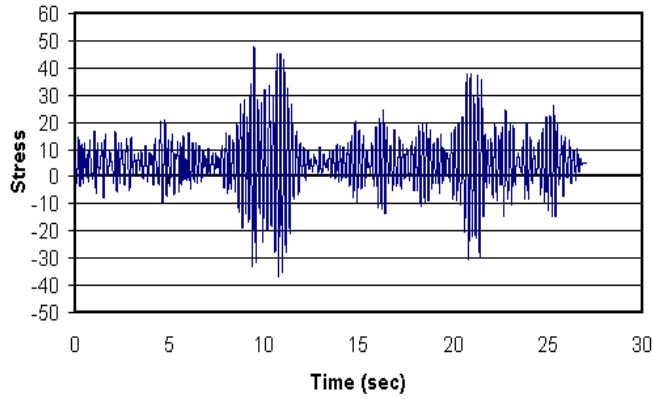


Figure 2.6: Variable amplitude fatigue loading: Spectrum loading [9]

The FALSTAFF (*F*ighter *A*ircraft *L*oading *S*Tandard *F*or *F*atigue) Loading sequence has been developed to represent the actual loads in the lower wing surface near the wing fuselage joint in tactical aircraft in an actual mission and is based on load factor and strain measurements from five such aircraft. There are many programs available for generating the load sequence for FE simulation/experimental use. The program used in this study is called Genesis and is developed by National Aerospace Laboratory (NLR), Netherlands [10]. The user interface is shown in Fig. 2.7. The program is capable of generating various load spectra including TWIST (*T*ransport *W*ing *S*Tandard), ENSTAFF (*E*Nvironmental *F*ALSTAFF), Helix (*H*inged rotor loading standard for Helicopters), Felix (*F*ixed rotor loading standard for Helicopters), WISPER (Standardized loading sequence for Wind turbines), TURBISTAN (Standardized loading sequence for fatigue of tactical aircraft engine discs). Genesis generates the entire load spectrum in terms of stress levels, which are also called reversal points.

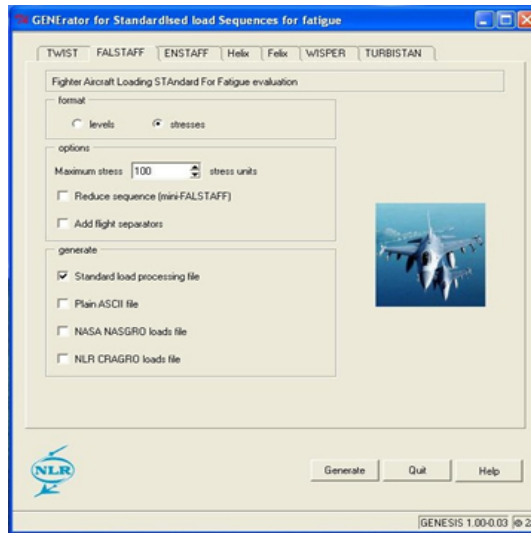


Figure 2.7: Genesis program user interface [10]

The standard FALSTAFF loading spectrum is comprised of 35966 reversal points. Fig. 2.8 shows the typical loading spectrum. The output text file from Genesis contains the list of stress levels

which are normalized based on user preferred stress level. In this study, the spectrum is such that maximum stress level is 100, which is further scaled to match a stress level of 250 MPa.

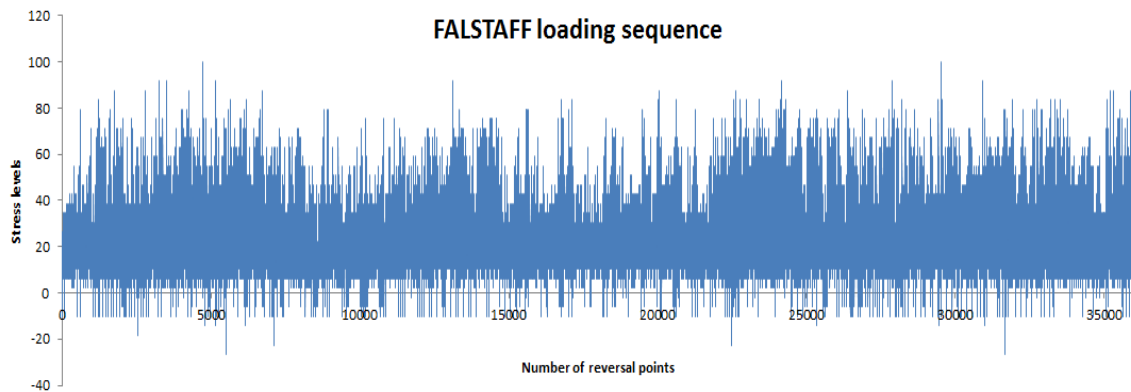


Figure 2.8: FALSTAFF Loading sequence

The Standard FALSTAFF sequence, as depicted in Fig. 2.8, has 1037 reversal points which are in compressive zone i.e. where the stress levels are below zero. To further simplify our experimental study, compressive stresses are made zero as to mainly avoid difficulty in testing. It is modified by a simple code written in MATLAB. Appendix A contains the MATLAB code for reference. The modified FALSTAFF loading sequence is depicted in Fig. 2.9. The lowest stress level in the modified load spectrum is kept at zero. The modified FALSTAFF load spectrum has 35655 number of reversal points. This load spectrum is then given as input to Zencrack 7.6 software for FEA simulation.

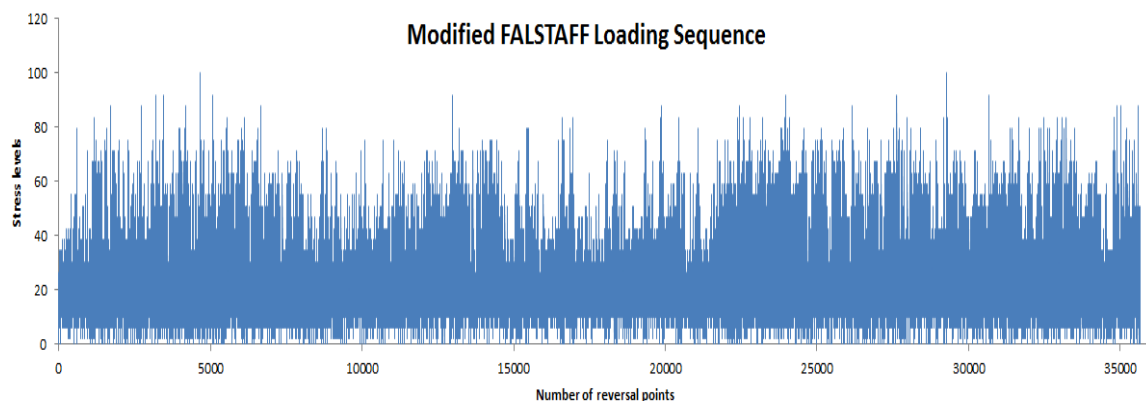


Figure 2.9: Modified FALSTAFF Loading sequence

## 2.4 Fatigue crack growth modelling using FEA

Finite element analysis is a powerful computational tool for conducting fatigue crack growth analysis. Present study uses Zencrack 7.6 interfaced with commercial FEA package ANSYS 12.1 for carrying out fatigue crack growth predictions under variable amplitude spectrum. Zencrack 7.6 software needs a FE mesh of the panel without any crack to be fed in to it as an input. Subsequent sections describe the model generation of SCC and CSC specimens in unrepaired, single sided repaired and double

sided repaired configurations in detail.

### 2.4.1 FEA Model Description

The uncracked meshed model of both SCC and CSC specimen are modelled in ANSYS 12.1 as per dimensions. Here, 8 noded SOLID 185 element is used for meshing. The final finite element built for both specimen types in unrepaired condition with out crack tip elements are shown in Fig. 2.10

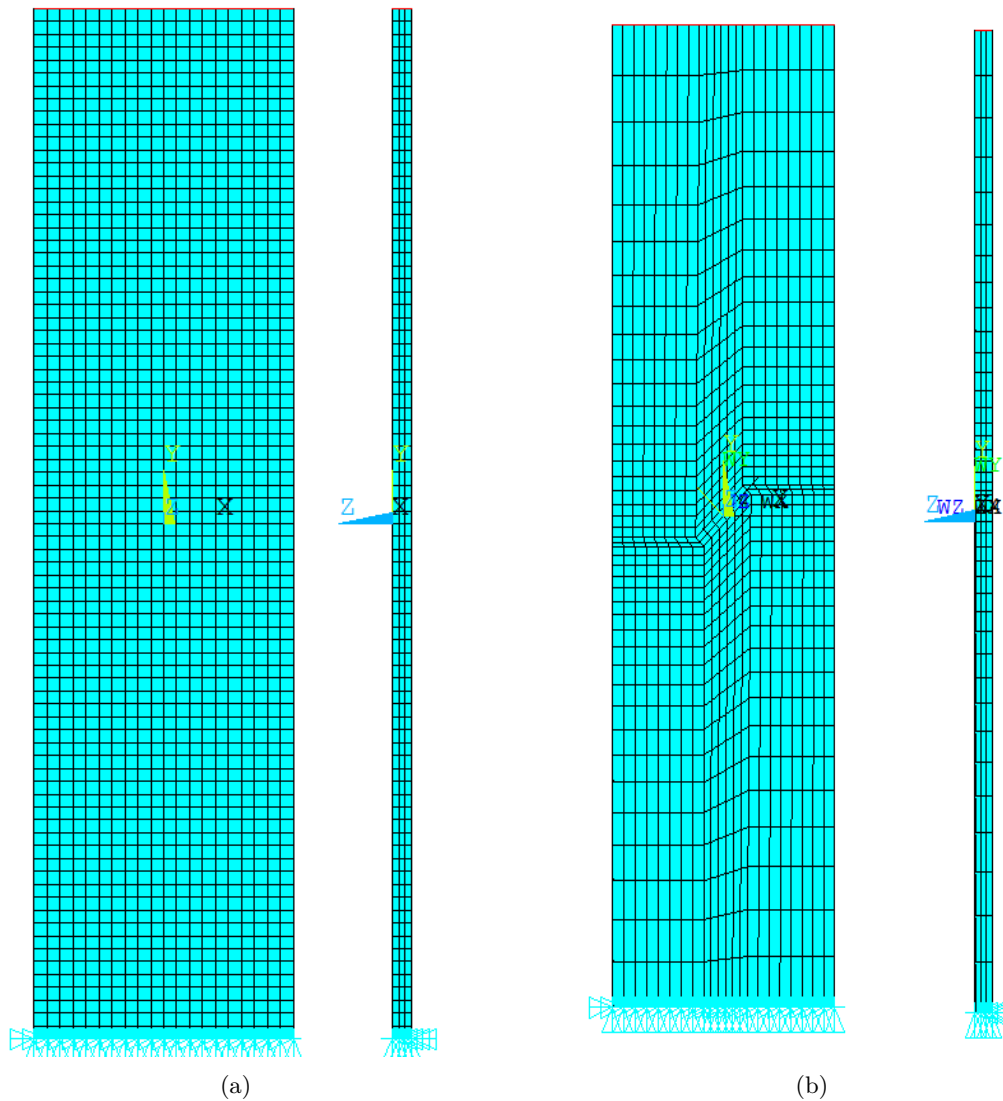


Figure 2.10: Finite element model of SCC and CSC specimens with out any crack tip elements (a) straight center crack (b) center slant crack

Figure 2.11 highlights the designated crack length and crack tips. The modelling of the crack front and crack surface is done in Zencrack 7.6 and is explained in section 2.4.4. Both FE mesh have 6 elements of element length 2 mm surrounding the crack. The thickness to the model is achieved by mesh is extruded in z-direction for 3 mm corresponding to intended Al 2014-T6 panel thickness and is made up of 3 elements along the z-direction.



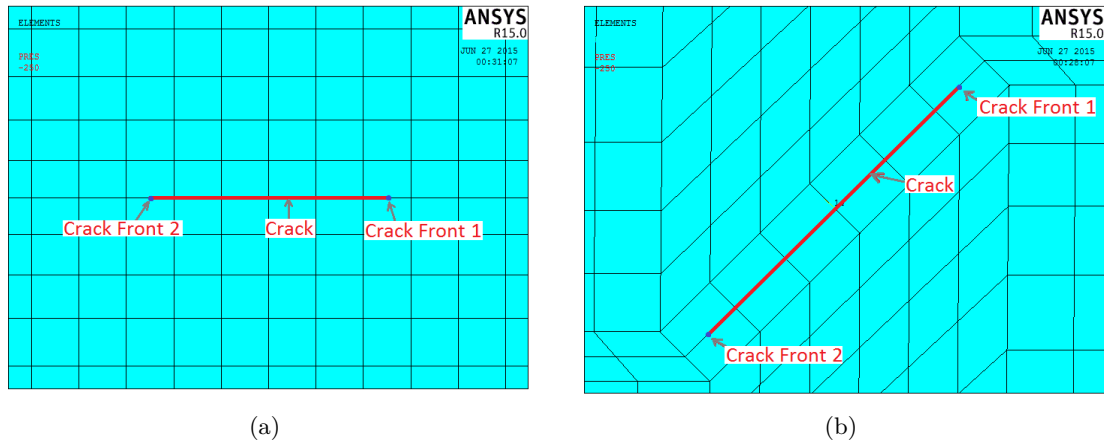


Figure 2.11: Zoomed in view of uncracked finite element model. (a) SCC specimen and (b) CSC specimen. Red lines designate the intended crack length which is going to be modelled by Zencrack 7.6

The basic FE model over the patch area in the panel is maintained same for the patch too. Further, in case of adhesively bonded patch repaired model both adhesive and patch are described in next section.

## 2.4.2 Patch Modelling- CZM

In fatigue crack growth study of repaired panel, modelling with adhesive layer is extremely important. Because in adhesively bonded joints, the adhesive interface between patch and aluminium panel is the weakest link which fails first under fatigue load. For modelling the interface, researchers in the past have proposed two criteria which try to predict the behaviour of adhesive layer. First one is Maximum shear stress criteria. In 2007, Papanikos et al. [32] used this criteria to model CFRP composite patch debonding from cracked metal sheet under static load involving approach. A recent study in 2013 by Toutanji et. al [40] have used this criteria to predict interfacial shear stress of externally bonded FRP to concrete substrate and theoretically determine the maximum transferable load. The criteria determines shear stress in the adhesive layer and degrades the properties of the adhesive layer element when a specified maximum shear stress is reached.

At the interface, cohesive zone is used to model the interface representing adhesive layer between panel and patch. With the increasing load, the cohesive zone surface which is intact before is separated by a distance due to the influence of high stress state at the interface especially at the overlap edge and over crack tip. The relation between the traction  $T$  and the separation  $\delta$  is defined as constitutive law for the cohesive zone surface. In this study, Bi-linear elastic-damage constitutive law for cohesive elements is used. After a critical elongation of  $\varepsilon_o$ , linear softening is proposed which is characterized by maximum traction and critical energy release rate. Ramji et al. [15] did a series of novel experiments to determine critical fracture energies that are required to model the cohesive modelling of adhesive interface. Energy release rate of this interface ( $G_{IC}$  and  $G_{IIC}$ ) at adhesive layer are defined in order to implement the debonding behaviour. Table 2.5 lists out the critical energy release rate for mode I and mode II. Adhesive stiffness is defined as  $k_I = E_a/t_a$  where  $E_a$  is the Young's modulus of the adhesive material and  $t_a$  is thickness of the adhesive layer. The degraded stiffness is denoted as  $k'$  and is defined as  $k' = (1/100)k$ .

Table 2.5: Adhesive material properties

Property	Araldite 2011
Stiffness ( $k_I$ )	11400N/mm
Fracture toughness in mode I	2.1N/mm
Fracture toughness in mode II	0.65N/mm
Stiffness after degradation ( $k'_I$ )	114N/mm

The FEA model of the repaired panel bonded along with the patch is shown in Fig. 2.12.

## 2.4.3 Introduction to Zencrack

Zencrack is a state-of-the-art software tool for 3D fracture mechanics simulation which allows fracture mechanics studies such as design of experiments, damage tolerance assessment, investigation of repair and maintenance, evaluation of residual life etc. to be completed in timely and effective manner. It uses FEA to calculate fracture mechanics parameters such as energy release rate, j-integral, CTOD and SIFs. Automatic generation of a cracked mesh out of user generated uncracked mesh enables Zencrack to calculate those fracture mechanics parameters. Next sections briefly explain the working of Zencrack 7.6.

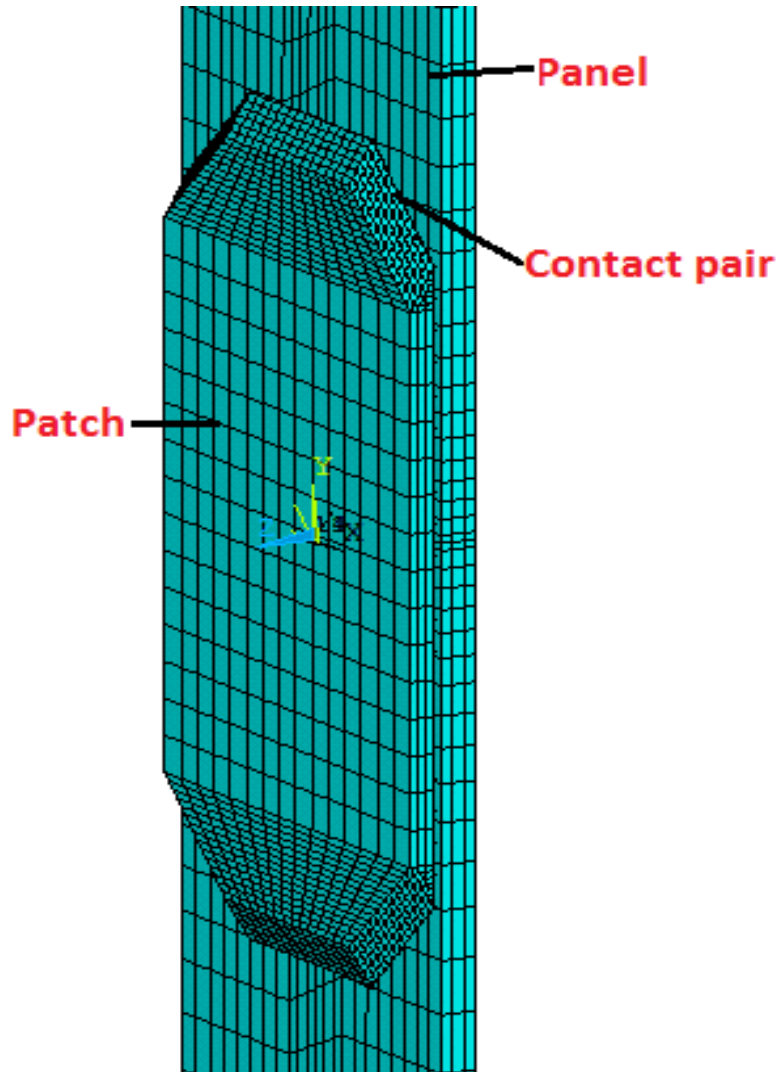


Figure 2.12: FEA model of composite patch

#### 2.4.4 Working of Zencrack

The uncracked mesh for the simulation is user created and Zencrack uses that uncracked mesh and converts it to a mesh with a crack by inserting one or more cracks into the uncracked mesh. This mesh is then submitted to finite element analysis. The results from the FEA are extracted and processed automatically to calculate fracture mechanics parameters. Crack front(s) in the mesh with the crack are advanced if the crack growth is modelled. The new mesh is again submitted to FEA and the process repeats until the analysis reaches a termination point e.g.  $K_{IC}$  is exceeded. Figure 2.13 shows a schematic diagram of the work flow of Zencrack. The key part of Zencrack working is creating mesh with a crack from user generated uncracked mesh. More details are in next section.

#### Crack block

A Crack-block approach is used to generate 3D meshes containing one or more crack fronts. Crack-block is nothing but a collection of brick elements stored as a unit cuboid. The arrangement of

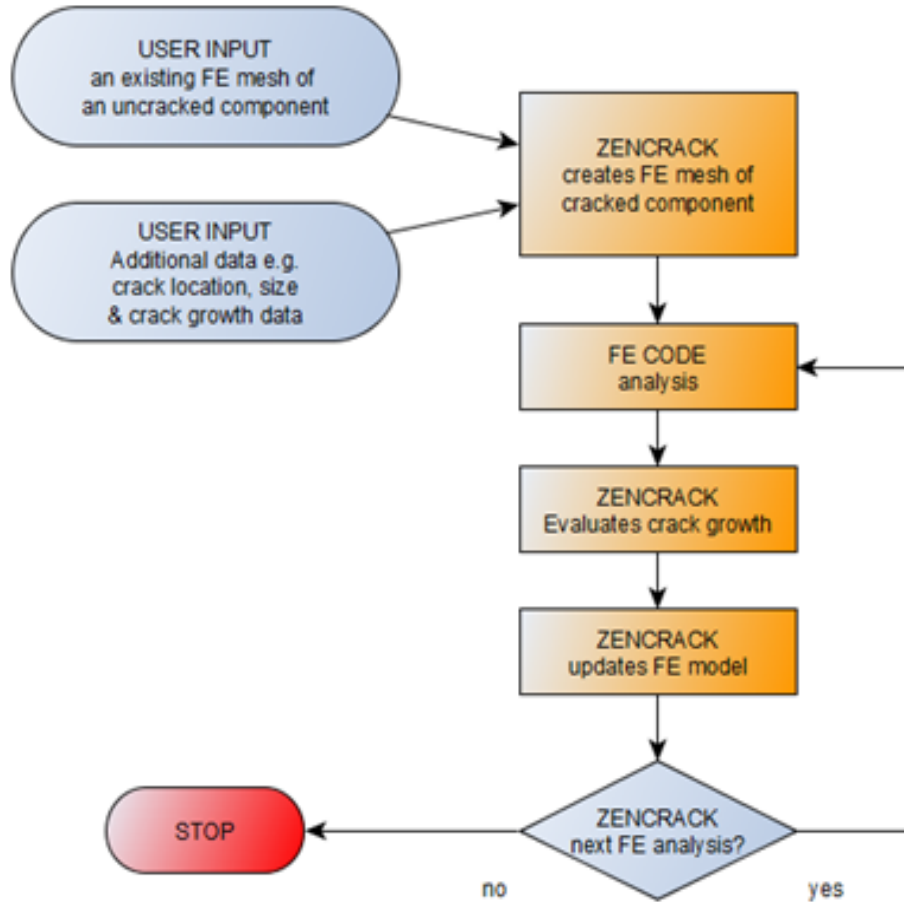


Figure 2.13: Working of Zencrack 7.6 [11]

the crack blocks is such that the unit cuboid form of the crack block contain a quarter circular or through crack front. Quarter circular crack block is generally used for surface cracks or corner cracks. Through crack block, as name suggests is used for through crack across the model. The elements around the crack front are arranged in rings to give a focussed mesh around the crack front. The particular crack block that this study uses is named as s02\_t19X1 and is shown in Fig. 2.14. The final mesh of unrepaired CSC panel after inserting the crack blocks looks like Fig. 2.15.

### Crack growth parameter estimation

As the crack growth is based on linear elastic fracture mechanics (LEFM) framework, the essential parameters such as SIF, crack propagation direction and crack growth need to be determined as the crack propagates. In this analysis, SIFs in all three modes are determined from the relative displacements of the pairs of modes on either side of the crack face in local mode I, II and III orientation. In order to achieve that, a local coordinate system is created as shown in Fig. 2.16. These relative displacements at the crack front are used to calculate SIFs and they are estimated using virtual crack closure technique (VCCT). The SIF expressions are given as Eqs. 2.2- 2.4.

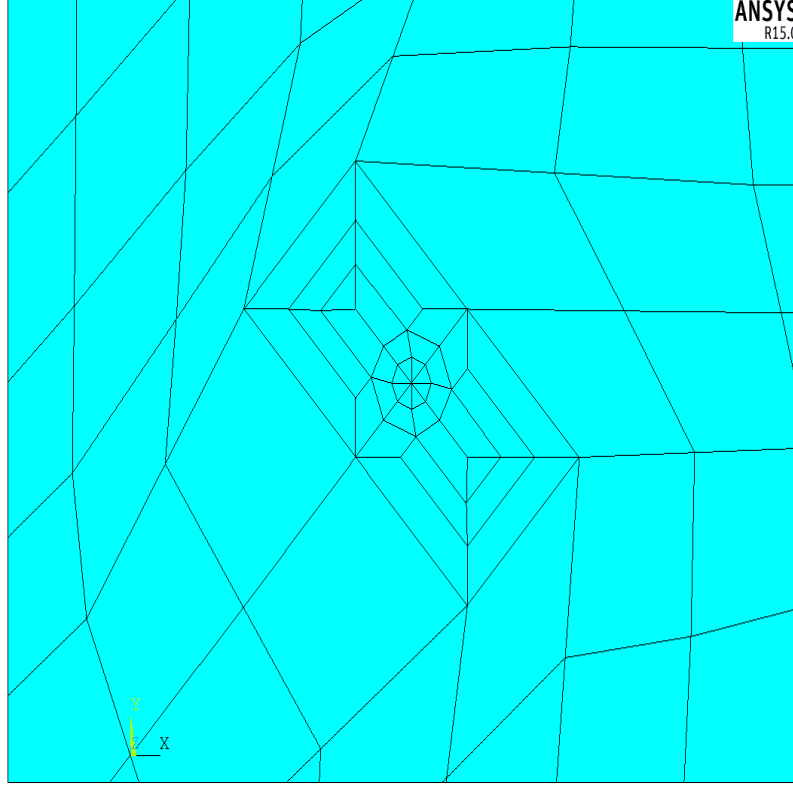


Figure 2.14: Crack block  $s02_t19x1$

$$K_I = \frac{EV_i}{4B} \sqrt{\frac{2\pi}{r}} \quad (2.2)$$

$$K_{II} = \frac{EV_{ii}}{4B} \sqrt{\frac{2\pi}{r}} \quad (2.3)$$

$$K_{III} = GV_{iii} \sqrt{\frac{\pi}{2r}} \quad (2.4)$$

$$B = 1 - \nu^2 \text{For planestrain} \quad (2.5)$$

$$B = 1 \text{For planestress} \quad (2.6)$$

$$G = \frac{E}{2(1 + \nu)} \quad (2.7)$$

For handling inclined crack, an equivalent energy release rate term is defined and it is estimated from stress intensity factors. This is defined in Eqn. 2.8.

$$G_{equiv} = \frac{B}{E}(K_I^2 + K_{II}^2) + \frac{1}{2G}K_{III}^2 \quad (2.8)$$

Upon simplification of Eqn. 2.8, one can re-write Eqn. 2.8 in terms of  $K_{eq}$  as shown in Eqn. 2.9.

$$K_{eq} = \sqrt{(K_I^2 + K_{II}^2) + (1 + \nu)K_{III}^2} \quad (2.9)$$

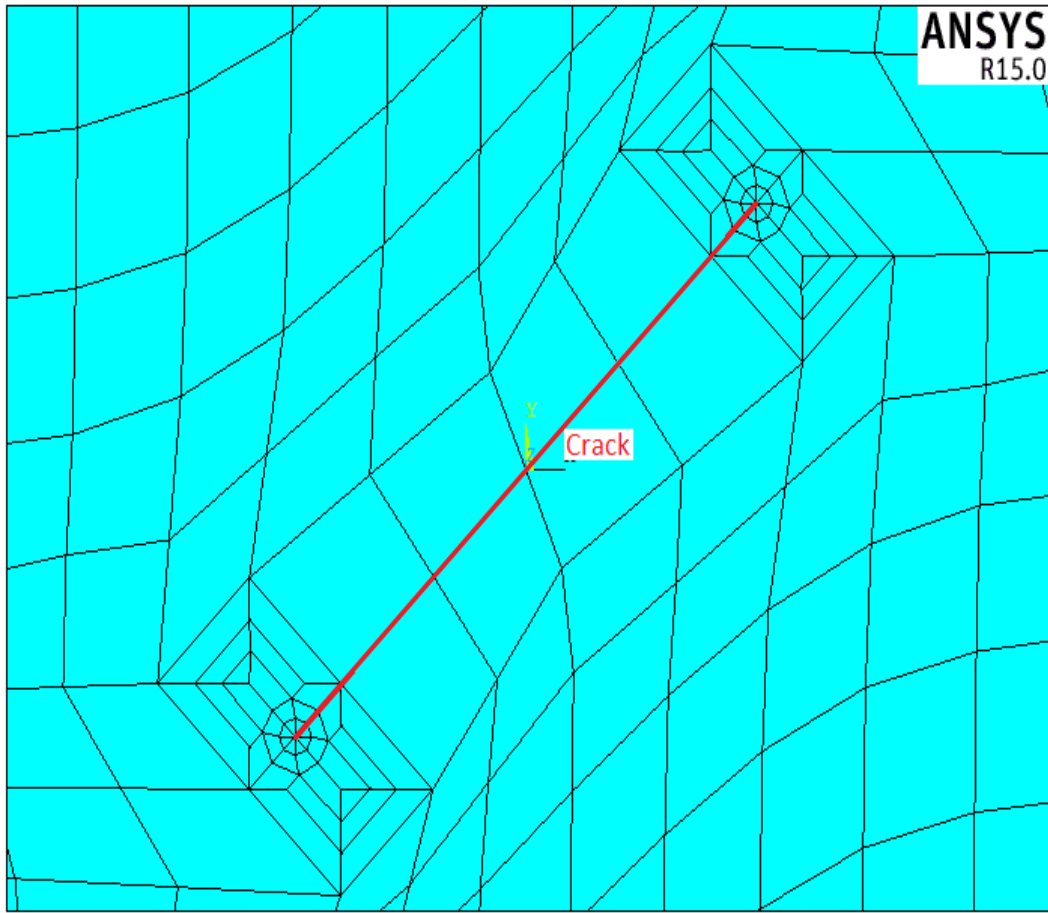


Figure 2.15: Mesh after crack block is inserted by Zencrack 7.6 software

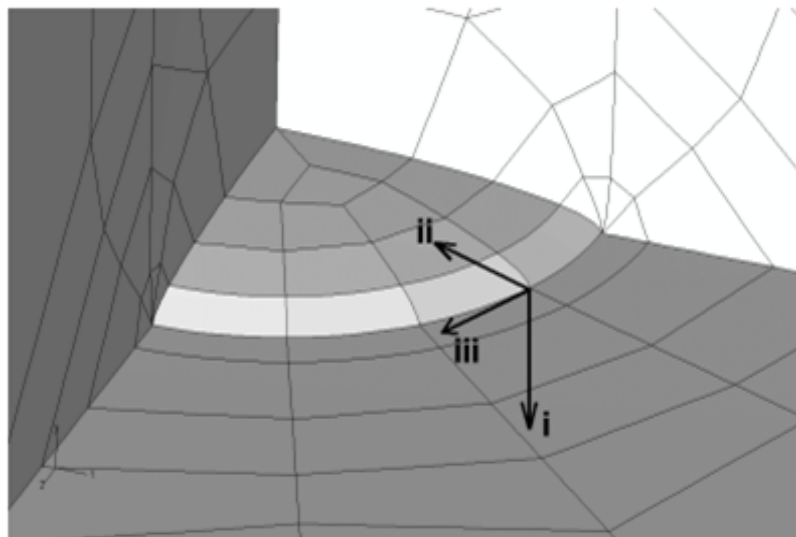


Figure 2.16: The local coordinate system is generated to measure crack opening displacements [11]

For any fatigue cycle, the difference between  $K_{eq}$  at maximum and minimum loading is defined as  $\Delta K_{eq}$  and can be expressed as Eqn. 2.10.

$$\Delta K_{eq} = (K_{eq})_{max} - (K_{eq})_{min} \quad (2.10)$$

Modified Paris' law is used to estimate the number of cycles. Upon substituting  $K_{eq}$  from Eqn. 2.10 in general Paris' law, one can get Eqn. 2.11. The material constants for crack growth estimations are taken from Table 2.4.

$$\Delta a \simeq C(\Delta K_{eq})^m \Delta N \quad (2.11)$$

In order to determine the new crack-front positions, crack propagation direction needs to be determined. There are many criteria available to calculate the crack propagation direction. In this study, maximum energy release rate criteria is used to estimate the crack growth direction. The crack growth direction is determined using the expressions in Eqns. 2.12, 2.13.

$$\left(\frac{dG_{ERR}}{d\theta}\right)_{\theta=\theta_o} = 0 \quad (2.12)$$

$$\left(\frac{dG_{ERR}^2}{d\theta^2}\right)_{\theta=\theta_o} \leq 0 \quad (2.13)$$

Energy release rate is numerically computed using virtual crack extension [11].

## 2.5 Results and Discussion

### 2.5.1 Fatigue life prediction

Figure 2.17 shows variation of fatigue life with crack length for unrepaired and repaired SCC panel. Figure 2.18 shows variation of fatigue life with crack length for unrepaired and repaired CSC panel. Blue curve represents the variation of unrepaired panel, red curve represents variation for single sided repaired panel, and green curve represents variation of double sided repaired panel. It is observed that the fatigue life is significantly improves for the repaired panel with CFRP patch, as reinforcement doesn't allow the crack tip to open under cyclic loading.

### 2.5.2 SIF Variation

Figure 2.19 shows the variation of stress intensity factors in mode I and II ( $K_I$  and  $K_{II}$ ) for SCC specimen against the crack length. Fig. 2.20 shows the same for CSC specimen. Fig. 2.19a shows the variation of  $K_I$  in SCC panel whereas Fig. 2.20a shows variation of  $K_I$  in CSC panel. Blue coloured line represents the variation for unrepaired panel, whereas red and green lines represent that for single sided and double sided repaired panels respectively. Similarly, the variation of  $K_{II}$  for both the panels are plotted in Figs. 2.19b and 2.20b respectively. As we can see in Figs. 2.19a and 2.20a,  $K_I$  increases with crack length as expected. Single sided and double sided repair provide a significant reduction in  $K_I$  value. The  $K_I$  in SCC panel is much higher from the beginning as the crack is straight and perpendicular to the loading direction, whereas the crack is inclined at  $45^\circ$  and it becomes perpendicular to loading eventually with increasing cycles. In both the panels,

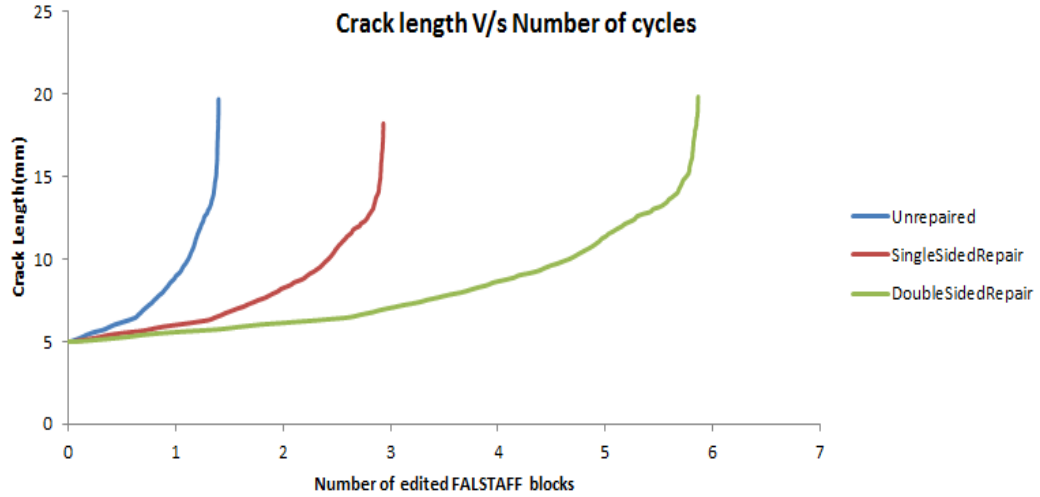


Figure 2.17: Crack length v/s number of modified FALSTAFF blocks for the SCC specimen obtained using FEA

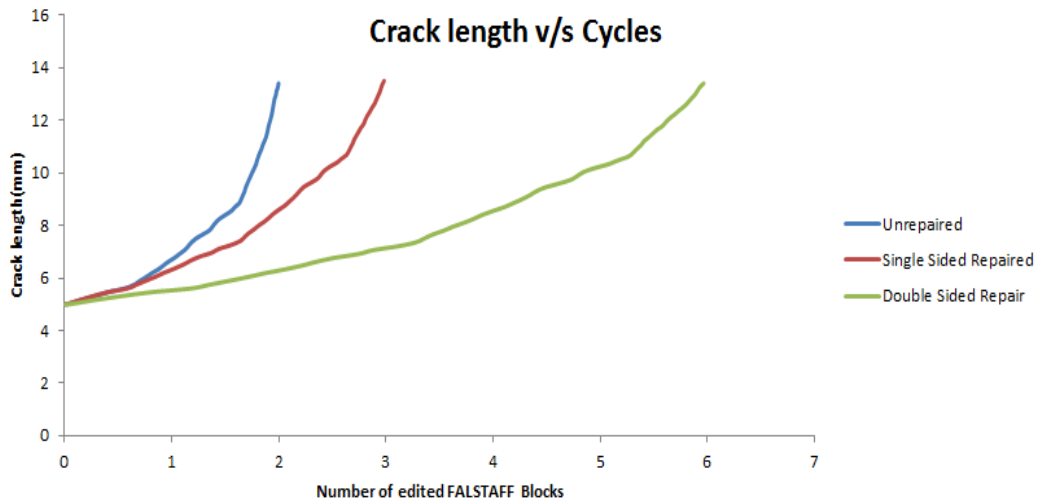


Figure 2.18: Crack length v/s number of modified FALSTAFF blocks for the CSC specimen obtained using FEA

$K_I$  in double sided repair is almost half of that as compared to single sided repaired panel. From Figs. 2.19b and 2.20b, we can observe that  $K_{II}$  decreases with increasing crack length, as it tends to propagate in perpendicular direction. In SCC panel,  $K_{II}$  is very low to begin because of the numerical instability. Further more, due to the additional bending stress being generated because of unsymmetrical nature of repair in single sided patch repair,  $K_{II}$  is observed to increase slightly after initial reduction.



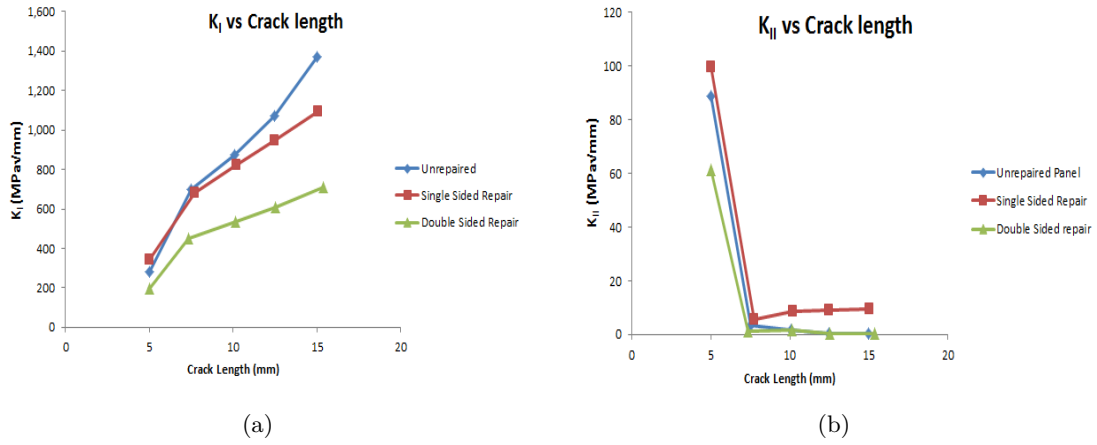


Figure 2.19: SIF variation for SCC panel. a:  $K_I$  variation; b:  $K_{II}$  variation

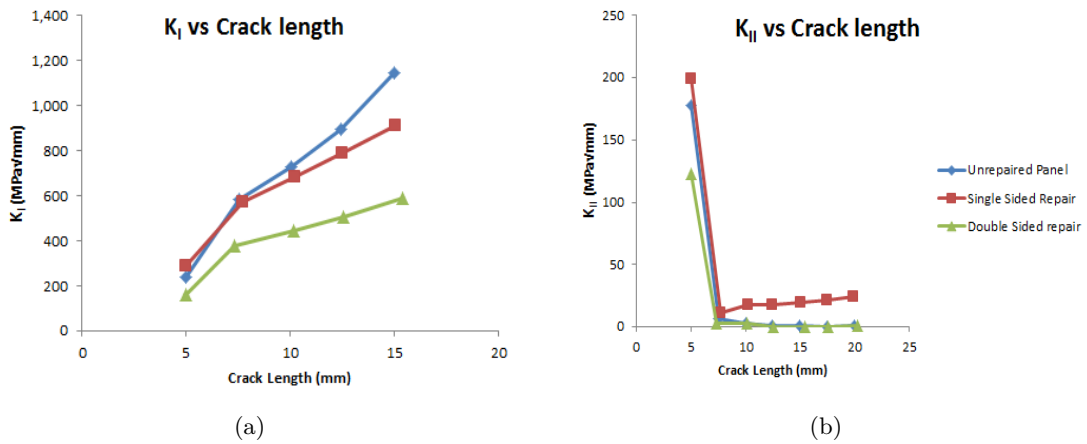


Figure 2.20: SIF variation for CSC panel. a:  $K_I$  variation; b:  $K_{II}$  variation

### 2.5.3 Crack front shapes

Figure 2.21 show the crack front shape over the crack plane as the crack tip advances with cycles. As one could see, an uniform crack front is observed in unrepaired and double sided repaired panel, whereas the crack front is unsymmetric in the case of single sided repaired panel. In single sided repaired panel, the crack grows at a faster rate on unpatched side as compared to the patched side. This non-uniform crack growth happens mainly due to additional bending phenomenon observed due to shift in neutral axis of single sided repaired panel. Further, for a given crack increment, double sided patch takes the maximum number of cycles as maximum reinforcement is present.

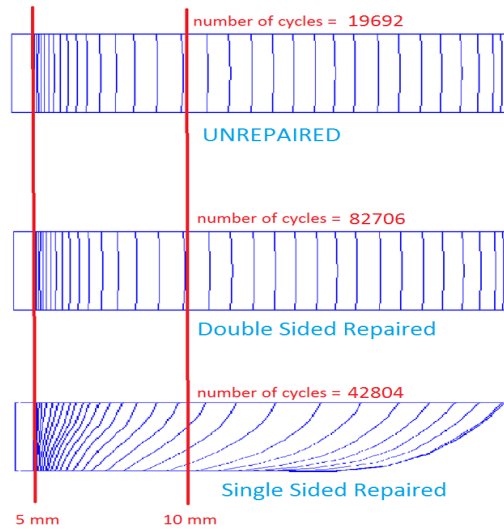


Figure 2.21: Crack front shapes and number of cycles corresponding to similar crack growth

## 2.6 Closure

In this chapter, fatigue crack growth study of straight center cracked (SCC) and center slant cracked (CSC) panels in unrepaired, single sided repaired and double sided repaired configurations is carried out using FEA. It is observed that composite patch repair shows a much improved fatigue life as compared to the unrepaired panel. It is also observed that double sided patch repaired panel has almost double the fatigue life than that of single sided patch repaired one. SIF variation is also studied using FEA. One could observe that  $K_I$  increases with the crack length in both SCC and CSC panels, whereas  $K_{II}$  decreases. Composite repair provide a significant reduction in SIFs as compared to unrepaired panel. Double sided repaired panel shows half the SIF value as compared to single sided repaired panel. The  $K_{II}$  value in single sided repaired panel increases slightly with the crack length due to additional asymmetry in case of the single sided repair resulting in bending stress part from in plane loading. This is also reflected in crack front shape as unrepaired and double sided repaired panel are having a symmetric crack front growth whereas single sided repair has unsymmetric crack front with increasing cycles.

## Chapter 3

# Experimental Investigation of Fatigue crack growth

In previous chapter, we have discussed the entire fatigue crack growth analysis using FEA. Therefore, a need exists to carry out the analysis using experimental tests to validate the results we have got from FEA. In this chapter, we will discuss the experimental method to verify the results for Straight center cracked specimen in unrepaired panel. Later, whole field strain analysis is carried out using digital image correlation (DIC) to measure the mode I stress intensity factor ( $K_I$ ) and compare it with the results obtained from the FEA study.

### 3.1 Specimen fabrication

In this section we will discuss the fabrication process for unrepaired SCC specimen. The panel is made up of 3mm thick aluminium AL 2014-T6 alloy sheet. The dog-bone specimen has the dimension as shown in figure 3.1. This line diagram is converted to cnc program and fed to EDM wire cutting machine, which cuts the sheet according to specimen dimensions. Then we have to drill a 2mm diameter hole in the center of the specimen using a HSS drill bit. After that we route the EDM wire through the hole and we program the EDM wire cut machine to cut a 4mm notch on opposite sides of the diameter of the hole, such that there is a 10mm crack length at the center of the specimen angled at  $0^\circ$ . This creates the initial notch for the SCC specimen.

The notch we just prepared has been cut by a 0.15 mm diameter wire, which is finite. To start a natural crack front we must first pre-crack the specimen. For pre-cracking procedure, freshly prepared specimen is loaded with a fatigue load on MTS servo-hydraulic testing machine. The fatigue load has target load of 3.85 kN and 3.15 amplitude. A liquid penetrant is applied inside the notch to make us enable to see if natural crack front is started. Approximately 15000 fatigue cycles are applied to start the natural crack front. This concludes the preparation of unrepaired SCC specimen. All that remains is to clean the specimen with isopropyl alcohol.

For DIC analysis, the surface is needed to be coated with a black speckle pattern. For that, first the specimen is cleaned with isopropyl alcohol and dried. Then the surface of the specimen is coated with a thin layer of white acrylic paint. With the help of airbrush, the specimen is sprayed with a carbon black paint from a fair distance, to generate a random black speckle pattern on the specimen.

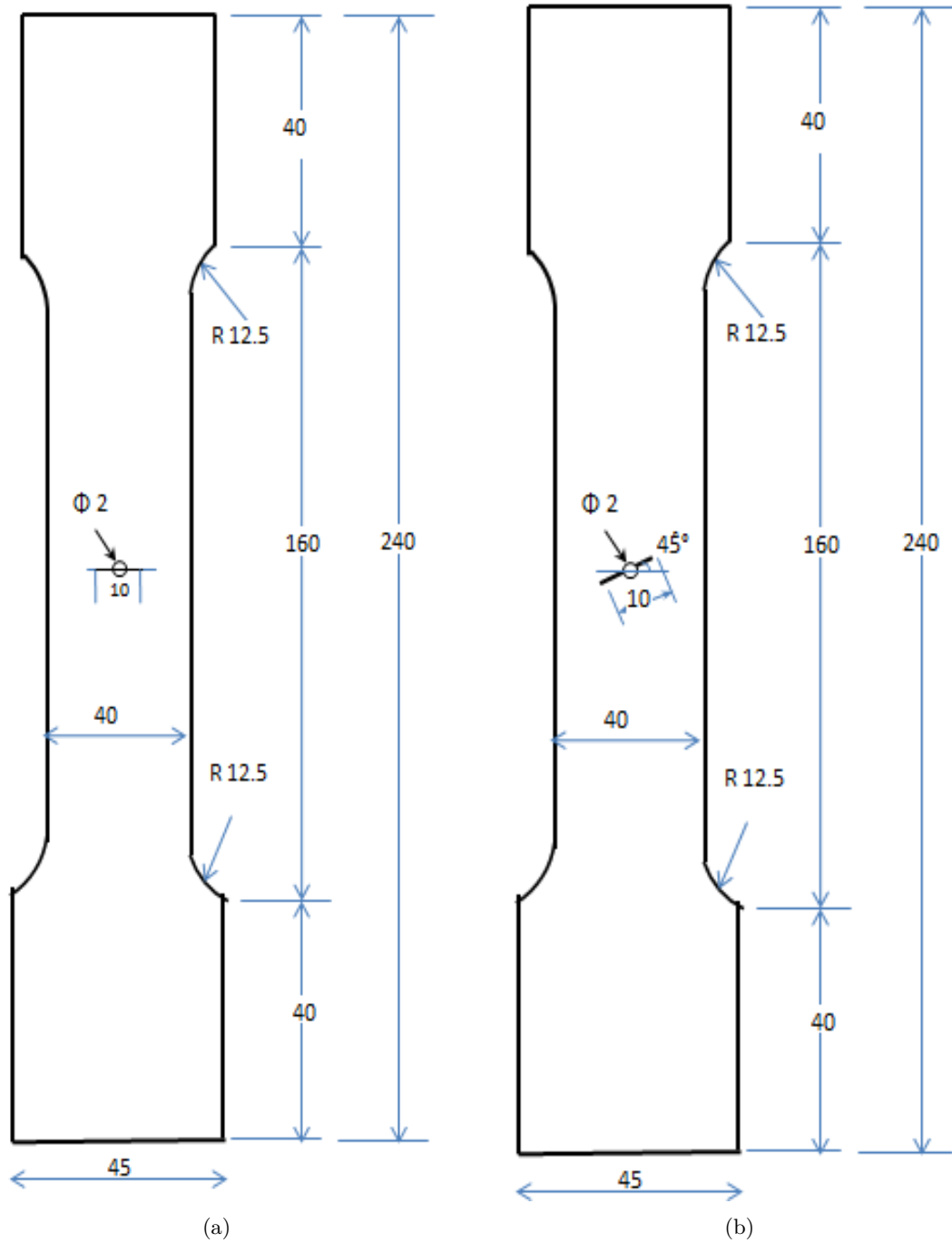


Figure 3.1: Line diagrams of the specimens: a) SCC specimen, b) CSC specimen

Figure 3.2 shows the speckle pattern near the notch. The back side of the panel is sprayed over with the acrylic white color, to measure the crack clearly by taking the pictures of the panel while being loaded. A small ruler is pasted to that side, to have a calibration scale for visual inspection of crack length.



Figure 3.2: Zoomed view of specimen showing the speckle pattern

## 3.2 Experimental Setup

After the specimen is fabricated, it is loaded in MTS servo-hydraulic testing machine with the help of 100 kN wedge grips on top and bottom. The pressure by which the specimen is held is kept at 500 PSI. The equipments for Digital Image correlation are setup around the MTS machine. The setup is depicted in figure 3.3.

There are 2 CCD cameras (POINTGREY-GRAS-50S5M-C) with Tamron zoom lens aligned perpendicular to the specimen on both sides (namely  $camera_0$  and  $camera_1$ ). Both of these cameras capture the images at a resolution of  $2448 \times 2048$  pixels.  $camera_0$  captures the specimen images from the back side, to enable us to measure the crack length properly, whereas  $camera_1$  captures the specimen from the front side, which is speckled for DIC analysis. Both of these cameras are controlled by the image capturing PC. Images are captured using commercial software VIC-snap. The images are captured at a frequency of 1 image per 2 minutes. Specimen is illuminated with two high intensity LED lights from both sides, which are controlled by a stroboscope controller. MTS machine controller and PC together control the MTS servo-hydraulic machine. The modified FALSTAFF loading is loaded up in the Multi-purpose testware software in MTS controlling PC. The loading is done at a 4 Hz frequency. The image grabbed are stored locally in image capturing PC. Examples of the grabbed images are shown in figure 3.4.



Figure 3.3: Experimental setup

### 3.3 Post-processing

After the images are captured during the experiment, they are post-processed for two outputs. One is crack length and other is mode I SIF at crack tip. For crack length analysis, images of the specimen from the back are studied. A MATLAB code is written in order to measure the distance from the notch tip to crack tip. The code also includes the calibration for converting the distance from pixel units to mm.

For measuring the SIF at crack tip, DIC analysis is performed. For performing DIC, we have used open source DIC code N-corr and in-house software SIF estimator. The images that are grabbed from the front side of the specimen (one with speckle pattern), are fed to N-corr. In that, every image is correlated with original reference image of the specimen with 0 load, to get strain field. The data generated is stored and used in SIF estimator. That program uses the strain field data from N-corr, materials data that we have already discussed, an original reference image, and approximate crack tip location to measure the SIF  $K_I$  at the crack tip.

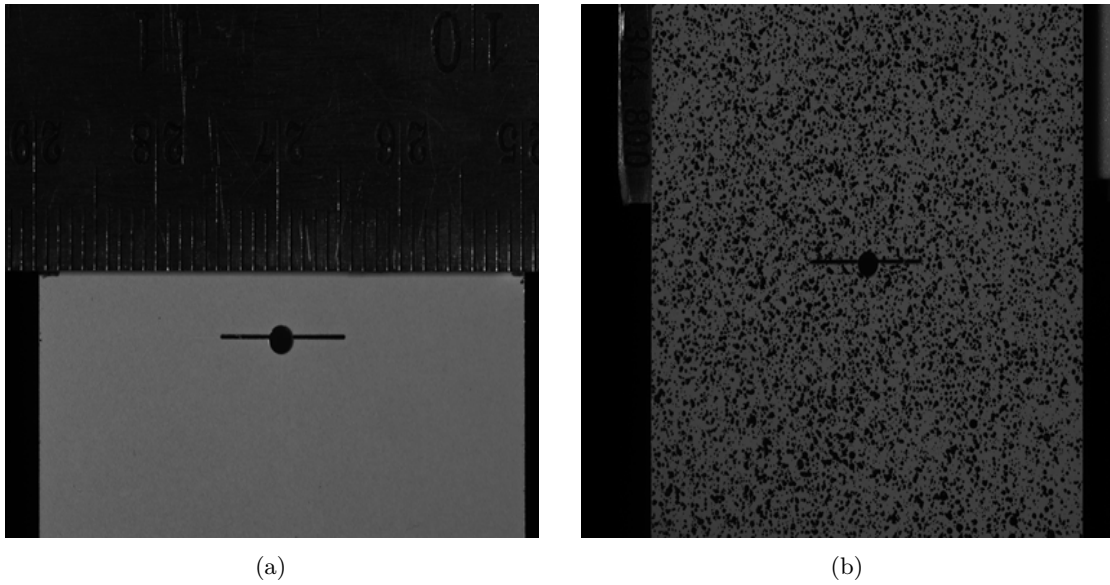


Figure 3.4: Examples of grabbed images a) from the back of the specimen, b) from the front of the specimen

### 3.4 Results and discussion

After we are done with post processing, the results are potted and compared against FEA. The crack length v/s number of cycles is potted in figure 3.5.

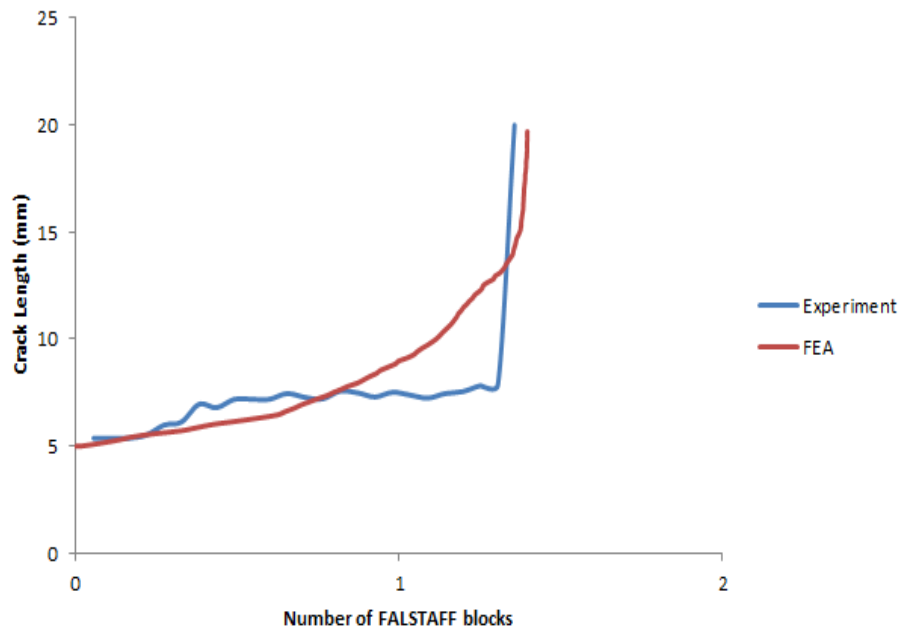


Figure 3.5: crack length versus Number of cycles plot

From the plot, we can observe that the final failure cycles of Experiment and FEA are comparable to each other. But in the experiment, the final failure is catastrophic. The crack grows slowly, then

it remains almost a constant value hovering around 7.3 mm and 7.8 mm before the final failure. Whereas FEA, the crack grows smoothly till the end. This difference in trend is observed because, FEA is based upon LEFM and ignores the plasticity effects arising due to overloads and underloads in FALSTAFF as it is a variable amplitude loading. The plasticity effects decrease the crack growth rate significantly in real life. The crack front shape is depicted in figure 3.6. Stress intensity factor we got from DIC analysis is depicted in plot 3.7 and it is compared with FEA values as well. As the graph is plotted against crack length and in experiment, crack length slowly increases upto around 7.8mm and then specimen catastrophically breaks, the experimental SIF plot is only upto that crack length, whereas we have SIF data for higher crack lengths in FEA.

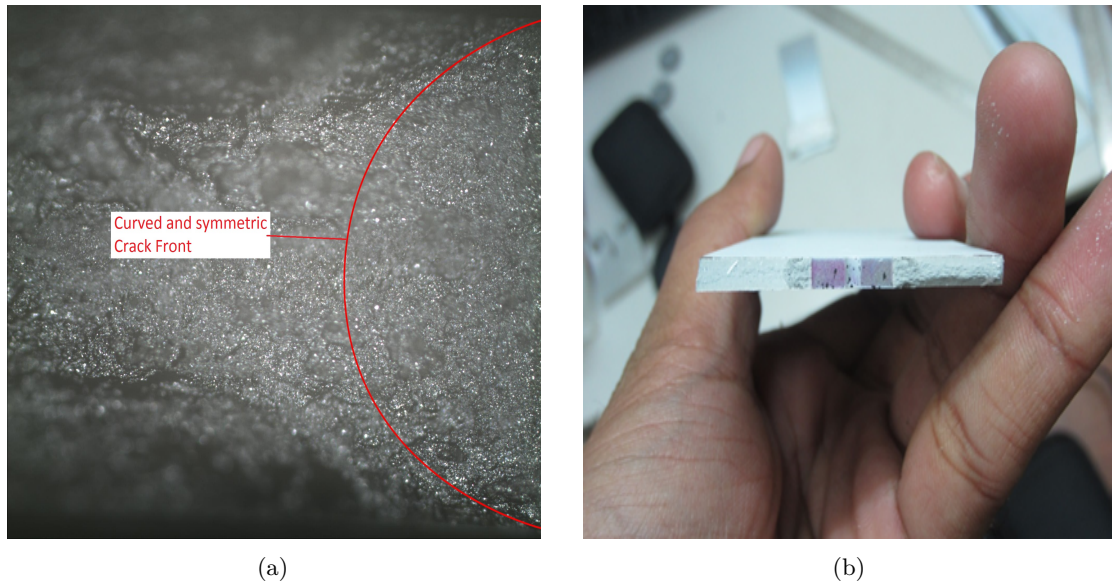


Figure 3.6: Shape of the crack front after failure of the specimen. a) A microscopic image; b) a macroscopic image

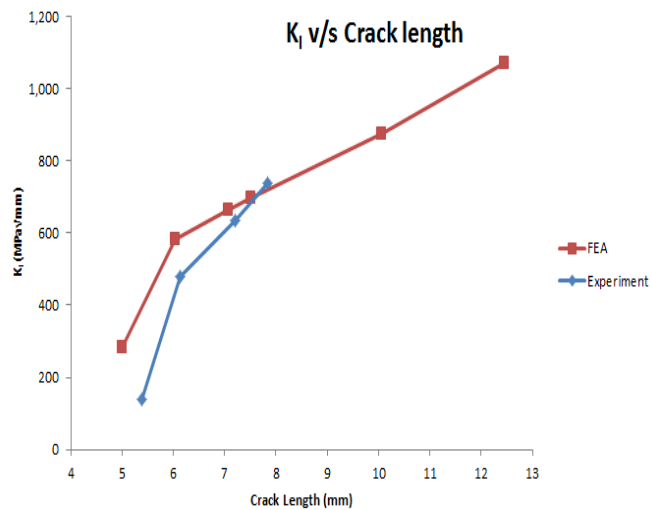


Figure 3.7:  $K_I$  versus crack length plot for experiment. It is also compared with FEA result.



### 3.5 Closure

In this chapter, a methodology has been discussed to verify the results obtained from FEA based study. The discussion included specimen fabrication, pre-cracking, loading and post-processing of the displacement field for SIF extraction. From the results, one can conclude that experimental results and FEA results are concurrent with each other. As in FEA study has not considered overload and underload effect occurring in variable amplitude loading, one could see a difference in the trend of crack growth. The final number of cycles are found to be comparable to each other. The SIF is also measured experimentally using DIC based technique and is compared to FEA prediction. Due to sudden failure of the specimen in experiment, one does not have enough data to compare with FEA prediction. The crack front shape in steady crack growth region is found to be a curved crack front with middle portion extending higher than those in final stages. The catastrophic failure is observed to have a  $45^\circ$  slant to the surface, which is expected from final fracture of the metallic specimen.

# Chapter 4

## Conclusions and Recommendations

### 4.1 Conclusions

Existing research work is mainly based upon study of mechanics of single and double sided patch repair applied on straight center cracked panel under tensile and constant amplitude fatigue loading. In actual situations, the damages occurring to aircraft structures are generally in mixed mode configuration and the loading under which the damages occur is generally a variable amplitude fatigue load. For repairing such damages, many repair techniques are implemented in real life and adhesively bonded composite patch repair technique is one of them. In this thesis, a numerical study is carried out to estimate the fatigue life of straight center cracked and center slant cracked aluminium Al 2014-T6 panel under modified FALSTAFF variable amplitude fatigue load. The results from the numerical study are also compared with experimental investigation carried on unrepaired center straight crack specimen.

In chapter 2, fatigue crack growth study is done under FALSTAFF variable amplitude fatigue loading using finite element analysis to estimate the fatigue crack growth life of straight center and center slant cracked specimens in unrepaired, single sided repaired and double sided repaired specimen. The variable amplitude fatigue loading applied is FALSTAFF load which was further modified to eliminate the control points in compressive zone. From the study, one could observe that the fatigue life of aluminium Al 2104-T6 panel was significantly improved when it is repaired with unidirectional CFRP patch. Further, it is observed that the fatigue life improvement in the double sided patch repair is almost double to that of single sided repaired panel. The adhesive modelling of the CFRP patch is done using cohesive zone modelling. The SIF variation of all three configurations are compared.  $K_I$  is observed to increase with the crack length. Mode 2 SIF  $K_{II}$  is observed to decrease as the crack length increased which is expected as crack tends to grow in perpendicular to the loading direction as number of cycle increase.

In chapter 3, experimental investigation is carried out to verify the results obtained from numerical study. The experiment was carried on unrepaired straight center cracked specimen. The fatigue loading is kept the same as FE analysis. The results that were obtained are observed to be concurrent with numerical study. The final failure was at a comparable number of cycles. But the failure trend observed is different in experiment. In experiment, the crack growth is constant upto a certain crack length and after that specimen failed catastrophically. The  $K_I$  values are also comparable to that of

FE analysis upto the sudden failure after which there is lack of availability of data to compare with FEA prediction.

From this study one can safely conclude that adhesively bonded composite patch repair technique is efficient. As the double sided patch repair was providing more fatigue life extension than that of single sided repair, whenever possible the double sided patch repair should be done.

## 4.2 Recommendations for future work

The results that are obtained from the FE analysis that was discussed in chapter 2 are based on linear elastic fracture mechanics (LEFM) framework. In LEFM framework, the plasticity effects arising from the overloading and underloading phenomenons repeatedly occurring in variable amplitude fatigue loading are not considered. Because of this, the fatigue crack growth is observed to be smooth till the final failure in contrary to catastrophic failure observed in experiment. There is a need to implement a different model for the numerical study which will incorporate these plasticity effects. The loading which is used is an modified version of FALSTAFF loading which is necessary simplify the experimental analysis. In future, actual FAISTAFF loading can be used to get more near-real-life results.

In experimental studies, the verification of results obtained from numerical studies for single sided and double sided repaired panel needs to be carried out which will give us more confidence on the results. Finding the exact crack tip location is always a difficult process to do and many times one gets inaccurate location. There is a need to find accurate crack tip location so that the SIF estimation can be done more efficiently. Finally, the image grabbing method that was implemented was a time based method which captured 1 image per 2 minutes. Because of this, peaks of the fatigue load are not captured effectively. Capturing the image at peaks can give us maximum crack opening displacement in the image which will enable us to find crack tip location more efficiently and SIF estimation would be more accurate.

## Appendix A

# Matlab Code to edit the FALSTAFF variable amplitude loading

For eliminating the control points in compressive zone, we have written a simple MATLAB code, which searches for points with negative stress level and replaces them with a value of zero.

The MATLAB code is given below and its working is discussed afterwards.

```
load FALSTAFF_stresses_plain_Original.txt
siz = size(FALSTAFF_stresses_plain_Original)
k=0;
for i=1:1:siz(1)
    if FALSTAFF_stresses_plain_Original(i)>= 0
        k=k+1;
        FALSTAFF_stresses_plain_Edited(k) = FALSTAFF_stresses_plain_Original(i);
    else
        k =k+1;
        FALSTAFF_stresses_plain_Edited(k) = 0;
    end
end

FALSTAFF_stresses_plain_Edited = FALSTAFF_stresses_plain_Edited';

siz2 = size(FALSTAFF_stresses_plain_Edited);

j = 1;
i=1;
while i < siz(1)
    if FALSTAFF_stresses_plain_Edited(i)~=0
```

```

        FALSTAFF_stresses_plain_Edited2(j) = FALSTAFF_stresses_plain_Edited(i);
        i=i+1
    else
        t=i;
        while FALSTAFF_stresses_plain_Edited(t+1)==0
            t=t+1;
        end
        FALSTAFF_stresses_plain_Edited2(j) = FALSTAFF_stresses_plain_Edited(i);
        i=t+1
    end
    j =j+1;

end

FALSTAFF_stresses_plain_Edited2 = FALSTAFF_stresses_plain_Edited2';

hold on
plot (FALSTAFF_stresses_plain_Edited2)
dlmwrite('FALSTAFF_stresses_plain_Edited.txt',FALSTAFF_stresses_plain_Edited2,'\n')

```

Figure A.1 shows the working of the code in a pictorial manner. First the code searches the text file with FALSTAFF loading for negative values. If found, the negative value is stored and the code loops to check if there are any more negative values after the first one. If no, then the code replaces the value with a zero. If yes, then ode loops till the first positive value and all of these negative values are joined as one zero value.

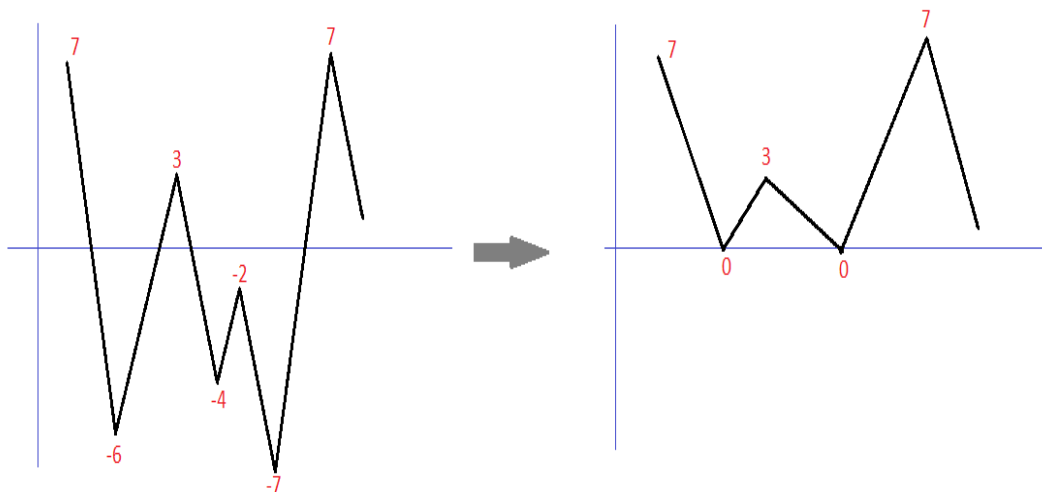


Figure A.1

# Appendix B

## Writing Zencrack Macro File

This appendix lists out and explains some important steps to write zencrack macro file, which in turn controls the FEA simulation.

1. For loading ANSYS APDL code file:

```
*FILES,UNCRAKED=unrep.ans
```

opens the file *unrep.ans*. It should be in the same folder as out macro file.

2. For replacing an element with a crack block:

```
s02_t19x1  
1384 1238 1243 1 1
```

Here, element number 1384 is being replaced by crack block *s02<sub>t</sub>19x1* such that crack is intended to grow in the direction of node number 1238 to 1243 and the crack front is situated at *1mm* from node 1238 and *1mm* from node 1243. For reference see figure B.1. The crack block *s02<sub>t</sub>19x1* looks like figure B.2

3. For splitting elements:

```
*SPLIT  
1378 1396
```

here, elements 1378 and 1396 are split so that Zencrack knows there is a crack in between those two elements. For reference, see figure B.3

4. for specifying the load

```
*LOAD SYSTEM,TYPE=spectrum, FILE=FALSTAFF_stresses_plain_Edited.sp3, SCALE=0.01  
0.05 1.00000E+00
```

here, we have specified the load as spectrum load, provided the file which contains the load spectrum. The scale normalizes the load values to desired values.

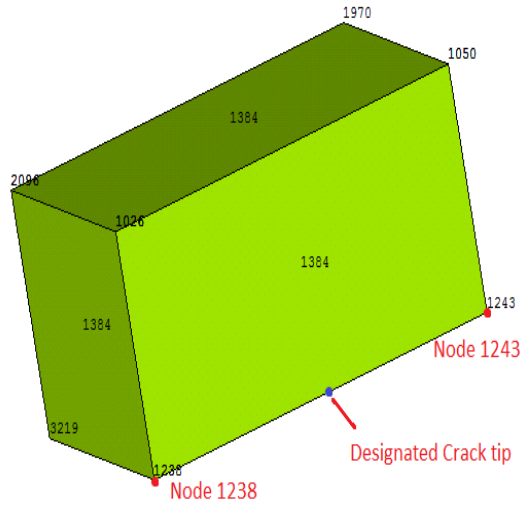


Figure B.1

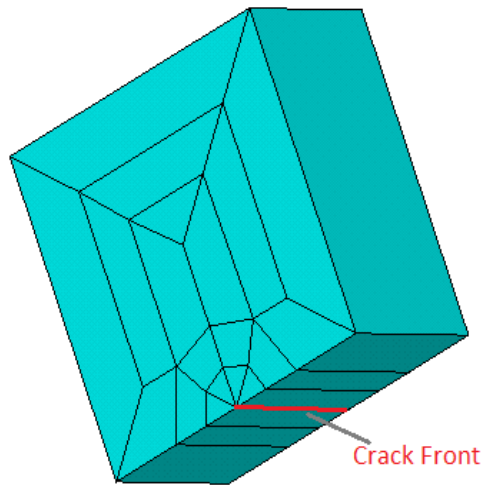


Figure B.2

5. For crack growth law specification

```
*CRACK GROWTH DATA,TYPE=PARIS,CONVERSION=1.00000
6.26e-13 3.30
```

here, we specify the crack growth law as Paris law. The Paris law constants are given on next line.

6. For giving the material properties:

```
*MATERIAL
73100,0.33,430,
```

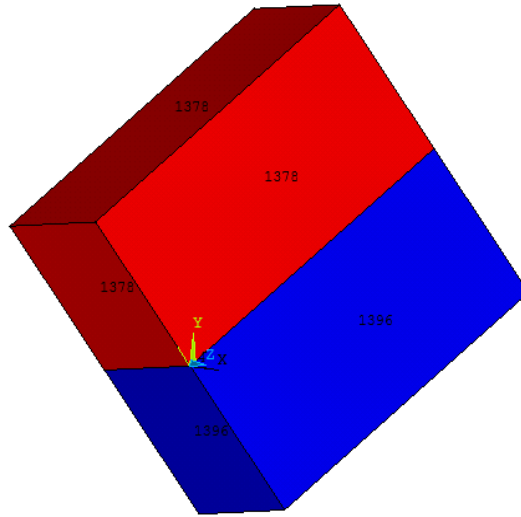


Figure B.3

Here, the important material properties such as Young's modulus, Poisson's ratio and Yield strength are provided.



# Appendix C

## Ansys 12.1 APDL codes

In this appendix, APDL codes which are used in the simulation are given for reference.

### C.1 APDL code for unrepaired panel

```
/COM, Structural
/PREP7
ET,1,185

*AFUN,DEG

!*ASK,tap,'ENTER tapered length '
!*ASK,n,'ENTER number of steps '
*SET,L,160
*SET,W,40
*SET,a,5
*SET,AA,10
*SET,THETA,45
*SET,ng1,6
*SET,n,0.04
*SET,PW,39

*SET,PL,70
*SET,n1,4
*SET,tap,PL/20
*SET,ts,3
*SET,ta,0.134
*SET,tp,2.1
*SET,G,PW/4
*SET,B,a+1
```

```

*SET,F, a*COS(THETA)
*SET,C, B*COS(THETA)
K, , , ,
K, ,W/2,C,,
K, ,W/2,L/2,,
K, ,-W/2,L/2,,
K, ,-W/2,-C,,
K, ,C,C,,
K, ,-C,-C,,
K, ,-W/2,-L/2,,
K, ,W/2,-L/2,,
LOCAL,14, , , ,45

```

```

K, ,B,1,,
K, ,B,-1,,

```

```

K, ,-B,-1,,
K, ,-B,1,,

```

```

CSYS,0
K, ,W/2, 4.949747468,,
K, ,W/2, 3.535533906,,

```

```

CSYS,14
K, ,,1,,
K, ,, -1,,
CSYS,0
K, ,-W/2,-4.949747468,,
K, ,-W/2, - 3.535533906 , ,

```

```

K, , -C ,L/2,,
K, , -F , -L/2,,
K, , F ,L/2,,
K, , C , -L/2,,
WPCSYS,-1,0
CSYS,0
FLST,2,7,3,ORDE,6
FITEM,2,1
FITEM,2,-2
FITEM,2,5

```

```

FITEM,2,-7
FITEM,2,16
FITEM,2,-17
KDELE,P51X
NUMCMP,KP
A,2,13,8,12
A,13,15,5,8
A,15,1,9,5
A,11,12,8,7
A,5,6,7,8
A,6,10,9,5
A,6,10,4,16
A,16,14,7,6
A,14,7,11,3
LOCAL,14,,,,45
LSEL,U,LOC,Y,-5,5
CSYS,0
LSEL,U,LOC,Y,L/2
LSEL,U,LOC,Y,-L/2
LSEL,U,LOC,Y,4.949747468
!*
LESIZE,ALL, , ,20,0.2, , , ,0

    FLST,5,2,4,ORDE,2
    FITEM,5,4
    FITEM,5,18
    CM,_Y1,LINE
    LSEL, , , ,P51X
    *GET,_z1,LINE, ,COUNT
    *SET,_z2,0
    *DO,_z5,1,_z1
    *SET,_z2,LSNEXT(_z2)
    *GET,_z3,LINE,_z2,ATTR,NDNX
    *GET,_z4,LINE,_z2,ATTR,SPNX
    *get,_z6,line,_z2,attr,kynd
    *IF,_z3,GT,0,THEN
    *IF,_z4,NE,0,THEN
    LESIZE,_z2, , ,_z3,1/_z4, , , ,_z6
    *ENDIF
    *ENDIF
    *ENDDO
    CMSEL,S,_Y1
    CMDELE,_Y1

```

```

alls,all
/REP,FAST
FLST,5,1,4,ORDE,1
FITEM,5,23
CM,_Y1,LINE
LSEL, , , ,P51X
*GET,_z1,LINE,,COUNT
*SET,_z2,0
*DO,_z5,1,_z1
*SET,_z2,LSNEXT(_z2)
*GET,_z3,LINE,_z2,ATTR,NDNX
*GET,_z4,LINE,_z2,ATTR,SPNX
*get,_z6,line,_z2,attr,kynd
*IF,_z3,GT,0,THEN
*IF,_z4,NE,0,THEN
LESIZE,_z2,,, _z3,1/_z4,,,,_z6
*ENDIF
*ENDIF
*ENDDO
CMSEL,S,_Y1
CMDELE,_Y1
ALLS,ALL
lsel,r,loc,x,4.949747468,W/2
LPLOT
LSEL,U,LOC,X,W/2
LESIZE,ALL, , , -1, ,1
LESIZE,ALL, , ,8, , , ,0

ALLS,ALL
lsel,r,loc,x,-4.949747468,-W/2
LPLOT
LSEL,U,LOC,X,-W/2
LESIZE,ALL, , , -1, ,1
LESIZE,ALL, , ,8, , , ,0

ALLS,ALL
LSEL,R,LOC,X,-4.949747468,4.949747468
LSEL,U,LOC,X,-4.949747468
LSEL,U,LOC,X,4.949747468
LPLOT
LESIZE,ALL, , ,6, , , ,0
ALLS,ALL
LSEL,R,,,11,17,6

```

```

lssel,a,,,12,14,2
LPLOT
LESIZE,ALL, , , -1, , 1
LESIZE,ALL, , , 2
ALLS,ALL

VEXT,ALL, , , 0,0,-3, , , ,

lssel,u,loc,z,0
lssel,u,loc,z,-3
lplo

LESIZE,ALL, , , 3, , , , 0
nsle
gplot
ALLS,ALL
VSWEEP,ALL

alls,all
cm,panel,elem
mp,ex,1,73100
mp,nuxy,1,0.33

nsle
nsel,r,loc,z,0
cm,c1,nodes
allsel,all
ALLS,ALL

alls,all
eplot
nsel,r,loc,y,-80
D,ALL, , 0, , , , ALL, , , , ,
ALLS,ALL
NSEL,R,LOC,Y,80
SF,ALL,PRES,-250

alls,all
nsle
eplot
FINISH

```

```

/SOLU
SOLVE
FINISH
/EXIT,SOLU

```

## C.2 APDL code for single sided repaired panel

```

/COM, Structural
/PREP7
ET,1,185

*AFUN,DEG
TB,CZM,6,,CBDE
TBDATA,1,28,2.1,20,.65
!*ASK,tap,'ENTER tapered length '
!*ASK,n,'ENTER number of steps '
*SET,L,160
*SET,W,40
*SET,a,5
*SET,AA,10
*SET,THETA,45
*SET,ng1,6
*SET,n,0.04
*SET,PW,38

*SET,PL,78
*SET,n1,4
*SET,tap,PL/20
*SET,ts,3
*SET,ta,0.134
*SET,tp,2.1
*SET,G,PW/4
*SET,B,a+1

*SET,F, a*COS(THETA)
*SET,C, B*COS(THETA)
K, , , ,
K, ,W/2,C, ,
K, ,W/2,L/2, ,
K, ,-W/2,L/2, ,
K, ,-W/2,-C, ,
K, ,C,C, ,

```

K, , -C, -C, ,  
K, , -W/2, -L/2, ,  
K, , W/2, -L/2, ,  
LOCAL, 14, , , , 45

K, , B, 1, ,  
K, , B, -1, ,

K, , -B, -1, ,  
K, , -B, 1, ,

CSYS, 0  
K, , W/2, 4.949747468, ,  
K, , W/2, 3.535533906, ,

CSYS, 14  
K, , , 1, ,  
K, , , -1, ,  
CSYS, 0  
K, , -W/2, -4.949747468, ,  
K, , -W/2, - 3.535533906 , ,

K, , -C , L/2, ,  
K, , -F , -L/2, ,  
K, , F , L/2, ,  
K, , C , -L/2, ,  
WPCSYS, -1, 0  
CSYS, 0  
FLST, 2, 7, 3, ORDE, 6  
FITEM, 2, 1  
FITEM, 2, -2  
FITEM, 2, 5  
FITEM, 2, -7  
FITEM, 2, 16  
FITEM, 2, -17  
KDELE, P51X  
NUMCMP, KP  
A, 2, 13, 8, 12  
A, 13, 15, 5, 8  
A, 15, 1, 9, 5

```

A,11,12,8,7
A,5,6,7,8
A,6,10,9,5
A,6,10,4,16
A,16,14,7,6
A,14,7,11,3
LOCAL,14,,,,45
LSEL,U,LOC,Y,-5,5
CSYS,0
LSEL,U,LOC,Y,L/2
LSEL,U,LOC,Y,-L/2
LSEL,U,LOC,Y,4.949747468
!*
LESIZE,ALL, , ,20,0.2, , , ,0

    FLST,5,2,4,ORDE,2
    FITEM,5,4
    FITEM,5,18
    CM,_Y1,LINE
    LSEL, , , ,P51X
    *GET,_z1,LINE,,COUNT
    *SET,_z2,0
    *DO,_z5,1,_z1
    *SET,_z2,LSNEXT(_z2)
    *GET,_z3,LINE,_z2,ATTR,NDNX
    *GET,_z4,LINE,_z2,ATTR,SPNX
    *get,_z6,line,_z2,attr,kynd
    *IF,_z3,GT,0,THEN
    *IF,_z4,NE,0,THEN
    LESIZE,_z2,,, _z3,1/_z4,,,,_z6
    *ENDIF
    *ENDIF
    *ENDDO
    CMSEL,S,_Y1
    CMDELE,_Y1
    alls,all
    /REP,FAST
    FLST,5,1,4,ORDE,1
    FITEM,5,23
    CM,_Y1,LINE
    LSEL, , , ,P51X
    *GET,_z1,LINE,,COUNT
    *SET,_z2,0

```



```

*DO, _z5, 1, _z1
*SET, _z2, LSNEXT(_z2)
*GET, _z3, LINE, _z2, ATTR, NDNX
*GET, _z4, LINE, _z2, ATTR, SPNX
*get, _z6, line, _z2, attr, kynd
*IF, _z3, GT, 0, THEN
*IF, _z4, NE, 0, THEN
LESIZE, _z2, , , _z3, 1/_z4, , , , _z6
*ENDIF
*ENDIF
*ENDDO
CMSEL, S, _Y1
CMDELE, _Y1
ALLS, ALL
lsel, r, loc, x, 4.949747468, W/2
LPLOT
LSEL, U, LOC, X, W/2
LESIZE, ALL, , , -1, , 1
LESIZE, ALL, , , 8, , , , 0

ALLS, ALL
lsel, r, loc, x, -4.949747468, -W/2
LPLOT
LSEL, U, LOC, X, -W/2
LESIZE, ALL, , , -1, , 1
LESIZE, ALL, , , 8, , , , 0

ALLS, ALL
LSEL, R, LOC, X, -4.949747468, 4.949747468
LSEL, U, LOC, X, -4.949747468
LSEL, U, LOC, X, 4.949747468
LPLOT
LESIZE, ALL, , , 6, , , , 0
ALLS, ALL
LSEL, R, , , 11, 17, 6
lsel, a, , , 12, 14, 2
LPLOT
LESIZE, ALL, , , -1, , 1
LESIZE, ALL, , , 2
ALLS, ALL

VEXT, ALL, , , 0, 0, -3, , , ,

```

```

lsel,u,loc,z,0
lsel,u,loc,z,-3
lplo

LESIZE,ALL,,3,,0
nsle
gplot
ALLS,ALL
VSWEEP,ALL

alls,all
cm,panel,elem
mp,ex,1,73100
mp,nuxy,1,0.3
emodif,all,mat,1

csys
vsel,r,volu,,1,9,1
nslv,r,1
cm,panel,elem
nsle
nsle
nsl,r,loc,z,0
cm,p1,nodes
allsel,all
ALLS,ALL
nsl,r,loc,z,-ts
cm,p2,nodes
alls,all
!adhesive modeling!!!!!!!!!!!!!!
k,51,(0.5*PW-G),(PL/2)
k,52,-(0.5*PW-G),(PL/2)
k,53,-PW/2,(0.5*PL-G)
k,54,PW/2,(0.5*PL-G)
k,55,-PW/2,-(0.5*PL-G)
k,56,(0.5*PW-G),-(PL/2)
k,57,-(0.5*PW-G),-(PL/2)
k,58,PW/2,-(0.5*PL-G)

A,51,52,53,54
A,55,57,56,58
A,54,58,55,53

```

```

aplot
asel,r,area,,43,45,1
VEXT,all,,0,0,ta,,,,
vsel,r,volu,,10,12,1
ASLV
lsla
lplot
lsel,u,loc,z,0
lsel,u,loc,z,ta
LESIZE,all,,1,,,,,0
alls,all
vsel,r,volu,,10,12,1
ASLV
lsla
lplot
lsel,r,loc,y,p1/2
lsel,a,loc,y,-p1/2
LESIZE,all,,15,,,,,0
alls,all
vsel,r,volu,,10,12,1
ASLV
lsla
lplot
lsel,r,loc,x,pw/2-g,pw/2

lsel,u,loc,x,pw/2
LESIZE,all,,5,,,,,0
alls,all
vsel,r,volu,,10,12,1
ASLV
lsla
lplot
lsel,r,loc,x,-(pw/2-g),-pw/2
lsel,u,loc,x,-pw/2
LESIZE,all,,5,,,,,0
alls,all
vsel,r,volu,,10,12,1
ASLV
lsla
lplot
lsel,r,loc,x,pw/2
lsel,a,loc,x,-pw/2
LESIZE,ALL,,20,,,,,0

```

```

ALLS,ALL

vsel,r,volu,,10,12,1
ASLV
lsla
lplot
lsel,r,loc,y,pl/2-G
lsel,a,loc,y,-(pl/2-G)
LESIZE,all,,15,,0
alls,all
vsel,r,volu,,10,12,1
vsweep,all

cmsel,u,panel
cm,adhesive,elem
mp,ex,2,1148
mp,nuxy,2,0.4
EMODIF,ALL,MAT,2,

vsel,r,volu,,10,12,1
nslv,r,1
allsel,below,volu
nset,r,loc,z,0

cm,ad1,nodes
alls,all
nsle
eplot
vsel,r,volu,,10,12,1
nslv,r,1
allsel,below,volu
nset,r,loc,z,ta
cm,ad2,nodes
allsel,all
nplot
alls,all
eplot
alls,all

!patch modeling!!!!!!!!!!!!!!!!!!!!!!

k,59,(0.5*PW-G),(PL/2),ta
k,60,-(0.5*PW-G),(PL/2),ta

```

```

k,61,-PW/2,(0.5*PL-G),ta
k,62,PW/2,(0.5*PL-G),ta
k,63,-PW/2,-(0.5*PL-G),ta
k,64,(0.5*PW-G),-(PL/2),ta
k,65,-(0.5*PW-G),-(PL/2),ta
k,66,PW/2,-(0.5*PL-G),ta

k,67,PW/2-G,-(0.5*PL-3.9),ta
k,68,-(PW/2-G),-(0.5*PL-3.9),ta
k,69,PW/2,-(0.5*PL-G-3.9),ta
k,70,-(PW/2),-(0.5*PL-G-3.9),ta

k,71,PW/2-G,(0.5*PL-3.9),ta
k,72,-(PW/2-G),(0.5*PL-3.9),ta
k,73,PW/2,(0.5*PL-G-3.9),ta
k,74,-(PW/2),(0.5*PL-G-3.9),ta
a,74,61,60,72
a,60,59,71,72
a,59,71,73,62
a,74,72,71,73
a,74,70,69,73
a,70,63,65,68
a,68,67,69,70
a,68,65,64,67
a,67,64,66,69

aplot
asel,r,area,,59,68,1
VEXT,all,,0,0,tp,,,,
a,59,62,47,46
a,59,46,44,60
a,60,44,41,61
a,64,78,50,66
a,64,78,77,65
a,63,49,77,65
VSBA,    14,    102
VSBA,    15,    101
VSBA,    13,    103
VSBA,    21,    104
VSBA,    20,    105
VSBA,    18,    106
vdele,23,28,,1

```

```

/rep
vsel,r,volu,,13,15,1
ASLV
lsla
lplot
lsel,u,loc,z,ta
lsel,u,loc,z,tp
LESIZE,all,,6,,0
alls,all
vsel,u,volu,,10,12,1
vsel,u,volu,,1,9,1
vsel,r,volu,,13,22,1
ASLV
LESIZE,ALL,,-1,,1
lplot
ASLV
lsla
lplot

lsel,r,loc,y,pw/2
lsel,a,loc,y,-pw/2
LESIZE,all,,10,,0
alls,all
vsel,r,volu,,13,22,1
ASLV
vsel,u,volu,,18
ASLV
lsla
lplot
LESIZE,ALL,,-1,,1
lsel,r,loc,x,pw/2-g,pw/2

lsel,u,loc,x,pw/2
LESIZE,all,,5,,0
alls,all
vsel,r,volu,,13,22,1
ASLV
vsel,u,volu,,18
ASLV
lsla
lplot
LESIZE,ALL,,-1,,1
lsel,a,loc,x,-(pw/2-g),-pw/2

```

```

lssel,u,loc,x,-pw/2
LESIZE,all,,5,,,,,0
alls,all
vsel,r,volu,,13,22,1
ASLV
vsel,u,volu,,18
ASLV
LESIZE,ALL,,,-1,,1
lplot
lsla
lplot
lssel,r,loc,x,pw/2
lssel,a,loc,x,-pw/2
LESIZE,all,,20,,,,,0
alls,all
vsel,r,volu,,13,22,1
ASLV
vsel,u,volu,,18
ASLV
LESIZE,ALL,,,-1,,1
lplot
lsla
lplot
lssel,r,loc,y,p1/2-G
lssel,a,loc,y,-(pL/2-G)
LESIZE,all,,10,,,,,0
alls,all
ALLS,ALL

ALLS,ALL
vsel,r,volu,,13,22,1
ASLV
vsel,u,volu,,18
ASLV
vsweep,all
cmsel,u,panel,elem
cmsel,u,adhesive,elem
cm,patch,elem
uimp,3,ex,ey,ez,81900,6150,6150
uimp,3,gxy,gyz,gxz,2770,2050,2770
uimp,3,prxy,pryz,prxz,0.34,0.5,0.34
EMODIF,ALL,MAT,3,
alls,all

```

```
eplot
ALLS,ALL
vsel,r,volu,,13,22,1
ASLV
vsel,u,volu,,18
ASLV
nslv,r,1
nset,r,loc,z,ta
cm,pd1,nodes
allsel,all
nsle
eplot
ALLS,ALL
vsel,r,volu,,13,22,1
ASLV
vsel,u,volu,,18
ASLV
eslv,r,1
```

```
cmsel,s,patch
nsle
eplot
local,11,0,0,0,0,90
emodif,all,esys,11
esys,0
csys,0
alls,all
nsle
eplot
```

!!!!!!!!!!!!!!bottom adhesive modeling!!!!!!!!!!!!!!

```
!!!!!!!!!!!!!!MPC CONTACT ALGORITHM!!!!!!!!!!!!!!
alls,all
eplot
/COM, CONTACT PAIR CREATION - START
CM,_NODECM,NODE
CM,_ELEMCM,ELEM
CM,_KPCM,KP
CM,_LINECM,LINE
CM,_AREACM,AREA
```



```

CM,_VOLUCM,VOLU
/GSAV,cwz,gsav,,temp
MP,MU,1,
MAT,6
MP,EMIS,2,7.88860905221e-31
R,3
REAL,3
ET,2,170
ET,3,174
R,3,,,-114,0.1,0,
RMORE,,1.0E20,0.0,1.0,-114
RMORE,0.0,0,1.0,,1.0,0.5
RMORE,0,1.0,1.0,0.0,,1.0
KEYOPT,3,4,0
KEYOPT,3,5,0
KEYOPT,3,7,0
KEYOPT,3,8,0
KEYOPT,3,9,0
KEYOPT,3,10,2
KEYOPT,3,11,0
KEYOPT,3,12,5
KEYOPT,3,2,0
KEYOPT,2,5,0
! Generate the target surface
NSEL,S,,P1
CM,_TARGET,NODE
TYPE,2
ESLN,S,0
ESURF
CMSEL,S,_ELEMCM
! Generate the contact surface
NSEL,S,,AD1
CM,_CONTACT,NODE
TYPE,3
ESLN,S,0
ESURF
ALLSEL
ESEL,ALL
ESEL,S,TYPE,,2
ESEL,A,TYPE,,3
ESEL,R,REAL,,3
/PSYMB,ESYS,1
/PNUM,TYPE,1

```

```

/NUM,1
EPLOT
ESEL,ALL
ESEL,S,TYPE,,2
ESEL,A,TYPE,,3
ESEL,R,REAL,,3
CMSEL,A,_NODECM
CMDEL,_NODECM
CMSEL,A,_ELEMCM
CMDEL,_ELEMCM
CMSEL,S,_KPCM
CMDEL,_KPCM
CMSEL,S,_LINECM
CMDEL,_LINECM
CMSEL,S,_AREACM
CMDEL,_AREACM
CMSEL,S,_VOLUCM
CMDEL,_VOLUCM
/GRES,cwz,gsav
CMDEL,_TARGET
CMDEL,_CONTACT
/COM, CONTACT PAIR CREATION - END
/COM, CONTACT PAIR CREATION - START
CM,_NODECM,NODE
CM,_ELEMCM,ELEM
CM,_KPCM,KP
CM,_LINECM,LINE
CM,_AREACM,AREA
CM,_VOLUCM,VOLU
/GSAV,cwz,gsav,,temp
MP,MU,1,0
MAT,6
MP,EMIS,2,7.88860905221e-31
R,4
REAL,4
ET,4,170
ET,5,174
R,4,,,-114,0.1,0,
RMORE,,1.0E20,0.0,1.0,-114
RMORE,0.0,0,1.0,,1.0,0.5
RMORE,0,1.0,1.0,0.0,,1.0
KEYOPT,5,4,0
KEYOPT,5,5,0

```

```

KEYOPT,5,7,0
KEYOPT,5,8,0
KEYOPT,5,9,0
KEYOPT,5,10,2
KEYOPT,5,11,0
KEYOPT,5,12,5
KEYOPT,5,2,0
KEYOPT,4,5,0
! Generate the target surface
NSEL,S,,AD2
CM,_TARGET,NODE
TYPE,4
ESLN,S,0
ESURF
CMSEL,S,_ELEMCM
! Generate the contact surface
NSEL,S,,PD1
CM,_CONTACT,NODE
TYPE,5
ESLN,S,0
ESURF
ALLSEL
ESEL,ALL
ESEL,S,TYPE,,4
ESEL,A,TYPE,,5
ESEL,R,REAL,,4
/PSYMB,ESYS,1
/PNUM,TYPE,1
/NUM,1
EPLLOT
ESEL,ALL
ESEL,S,TYPE,,4
ESEL,A,TYPE,,5
ESEL,R,REAL,,4
CMSEL,A,_NODECM
CMDEL,_NODECM
CMSEL,A,_ELEMCM
CMDEL,_ELEMCM
CMSEL,S,_KPCM
CMDEL,_KPCM
CMSEL,S,_LINECM
CMDEL,_LINECM
CMSEL,S,_AREACM

```

```
CMDEL,_AREACM
CMSEL,S,_VOLUCM
CMDEL,_VOLUCM
/GRES,cwz,gsav
CMDEL,_TARGET
CMDEL,_CONTACT
/COM, CONTACT PAIR CREATION - END
```

```
alls,all
eplot
nselect,r,loc,y,-80
D,ALL,,0,,,ALL,,,,,
ALLS,ALL
NSEL,R,LOC,Y,80
SF,ALL,PRES,-250
alls,all
```

```
eset,s,adj,,2789
nsle
eplot
emodif,all,mat,2
/rep
alls,all
nsle
eplot
```

```
eset,s,adj,,5293
nsle
eplot
emodif,all,mat,3
emodif,all,esys,11
```

```
alls,all
eset,s,adj,,1793
nsle
eplot
cm,panel,elems
nsle
eplot
emodif,all,mat,1
alls,all
nsle
eplot
```

```

FINISH
/SOLU
SOLVE
FINISH
/EXIT,SOLU

```

### C.3 APDL code for double sided repaired panel

```

/COM, Structural
/PREP7
ET,1,185

*AFUN,DEG
TB,CZM,6,,,CBDE
TBDATA,1,28,2.1,19,0.65
!*ASK,tap,'ENTER tapered length '
!*ASK,n,'ENTER number of steps '
*SET,L,160
*SET,W,40
*SET,a,5
*SET,AA,10
*SET,THETA,45
*SET,ng1,6
*SET,n,0.04
*SET,PW,38

*SET,PL,78
*SET,n1,4
*SET,tap,PL/20
*SET,ts,3
*SET,ta,0.134
*SET,tp,2.1
*SET,G,PW/4
*SET,B,a+1

*SET,F, a*COS(THETA)
*SET,C, B*COS(THETA)
K, , , ,
K, ,W/2,C,,
K, ,W/2,L/2,,
K, ,-W/2,L/2,,
K, ,-W/2,-C,,

```

K, ,C,C,,  
K, ,-C,-C,,  
K, ,-W/2,-L/2,,  
K, ,W/2,-L/2,,  
LOCAL,14,,,,,45

K, ,B,1,,  
K, ,B,-1,,

K, ,-B,-1,,  
K, ,-B,1,,

CSYS,0  
K, ,W/2, 4.949747468,,  
K, ,W/2, 3.535533906,,

CSYS,14  
K, ,,1,,  
K, ,, -1,,  
CSYS,0  
K, ,-W/2,-4.949747468,,  
K, ,-W/2, - 3.535533906 ,,

K, , -C ,L/2,,  
K, , -F , -L/2,,  
K, , F ,L/2,,  
K, , C , -L/2,,  
WPCSYS,-1,0  
CSYS,0  
FLST,2,7,3,ORDE,6  
FITEM,2,1  
FITEM,2,-2  
FITEM,2,5  
FITEM,2,-7  
FITEM,2,16  
FITEM,2,-17  
KDELE,P51X  
NUMCMP,KP  
A,2,13,8,12  
A,13,15,5,8

```

A,15,1,9,5
A,11,12,8,7
A,5,6,7,8
A,6,10,9,5
A,6,10,4,16
A,16,14,7,6
A,14,7,11,3
LOCAL,14,,,,,45
LSEL,U,LOC,Y,-5,5
CSYS,0
LSEL,U,LOC,Y,L/2
LSEL,U,LOC,Y,-L/2
LSEL,U,LOC,Y,4.949747468
!*
LESIZE,ALL, , ,20,0.2, , , ,0

    FLST,5,2,4,ORDE,2
    FITEM,5,4
    FITEM,5,18
    CM,_Y1,LINE
    LSEL, , , ,P51X
    *GET,_z1,LINE,,COUNT
    *SET,_z2,0
    *DO,_z5,1,_z1
    *SET,_z2,LSNEXT(_z2)
    *GET,_z3,LINE,_z2,ATTR,NDNX
    *GET,_z4,LINE,_z2,ATTR,SPNX
    *get,_z6,line,_z2,attr,kynd
    *IF,_z3,GT,0,THEN
    *IF,_z4,NE,0,THEN
    LESIZE,_z2,,,_z3,1/_z4,,,,_z6
    *ENDIF
    *ENDIF
    *ENDDO
    CMSEL,S,_Y1
    CMDELE,_Y1
    alls,all
    /REP,FAST
    FLST,5,1,4,ORDE,1
    FITEM,5,23
    CM,_Y1,LINE
    LSEL, , , ,P51X
    *GET,_z1,LINE,,COUNT

```

```

*SET,_z2,0
*DO,_z5,1,_z1
*SET,_z2,LSNEXT(_z2)
*GET,_z3,LINE,_z2,ATTR,NDNX
*GET,_z4,LINE,_z2,ATTR,SPNX
*get,_z6,line,_z2,attr,kynd
*IF,_z3,GT,0,THEN
*IF,_z4,NE,0,THEN
LESIZE,_z2,,,_z3,1/_z4,,,,_z6
*ENDIF
*ENDIF
*ENDDO
CMSEL,S,_Y1
CMDELE,_Y1
ALLS,ALL
lsel,r,loc,x,4.949747468,W/2
LPLOT
LSEL,U,LOC,X,W/2
LESIZE,ALL,,,-1,,1
LESIZE,ALL,,8,,,,,0

ALLS,ALL
lsel,r,loc,x,-4.949747468,-W/2
LPLOT
LSEL,U,LOC,X,-W/2
LESIZE,ALL,,,-1,,1
LESIZE,ALL,,8,,,,,0

ALLS,ALL
LSEL,R,LOC,X,-4.949747468,4.949747468
LSEL,U,LOC,X,-4.949747468
LSEL,U,LOC,X,4.949747468
LPLOT
LESIZE,ALL,,6,,,,,0
ALLS,ALL
LSEL,R,,,11,17,6
lsel,a,,,12,14,2
LPLOT
LESIZE,ALL,,,-1,,1
LESIZE,ALL,,,2
ALLS,ALL

```



```

VEXT,ALL, , ,0,0,-3,,,

lsel,u,loc,z,0
lsel,u,loc,z,-3
lplo

LESIZE,ALL, , ,3, , , ,0
nsle
gplot
ALLS,ALL
VSWEEP,ALL

alls,all
cm,panel,elem
mp,ex,1,73100
mp,nuxy,1,0.3
emodif,all,mat,1

csys
vsel,r,volu, ,1,9,1
nslv,r,1
cm,panel,elem
nsle
nsle
nsl,r,loc,z,0
cm,p1,nodes
allsel,all
ALLS,ALL
nsl,r,loc,z,-ts
cm,p2,nodes
alls,all
!adhesive modeling!!!!!!!!!!!!!!
k,51,(0.5*PW-G),(PL/2)
k,52,-(0.5*PW-G),(PL/2)
k,53,-PW/2,(0.5*PL-G)
k,54,PW/2,(0.5*PL-G)
k,55,-PW/2,-(0.5*PL-G)
k,56,(0.5*PW-G),-(PL/2)
k,57,-(0.5*PW-G),-(PL/2)
k,58,PW/2,-(0.5*PL-G)

A,51,52,53,54
A,55,57,56,58

```

```

A,54,58,55,53
aplot
asel,r,area,,43,45,1
VEXT,all,, ,0,0,ta,,,
vsel,r,volu,,10,12,1
ASLV
lsla
lplot
lsel,u,loc,z,0
lsel,u,loc,z,ta
LESIZE,all,, ,1, , , ,0
alls,all
vsel,r,volu,,10,12,1
ASLV
lsla
lplot
lsel,r,loc,y,p1/2
lsel,a,loc,y,-p1/2
LESIZE,all,, ,15, , , ,0
alls,all
vsel,r,volu,,10,12,1
ASLV
lsla
lplot
lsel,r,loc,x,pw/2-g,pw/2

lsel,u,loc,x,pw/2
LESIZE,all,, ,5, , , ,0
alls,all
vsel,r,volu,,10,12,1
ASLV
lsla
lplot
lsel,R,loc,x,-(pw/2-g),-pw/2
lsel,u,loc,x,-pw/2
LESIZE,all,, ,5, , , ,0
alls,all
vsel,r,volu,,10,12,1
ASLV
lsla
lplot
lsel,r,loc,x,pw/2
lsel,a,loc,x,-pw/2

```

```

LESIZE,ALL, , ,20, , , , ,0
ALLS,ALL

vsel,r,volu, ,10,12,1
ASLV
lsla
lplot
lsel,r,loc,y,pl/2-G
lsel,a,loc,y,-(pl/2-G)
LESIZE,all, , ,15, , , , ,0
alls,all
vsel,r,volu, ,10,12,1
vsweep,all

cmsel,u,panel
cm,adhesive,elem
mp,ex,2,1148
mp,nuxy,2,0.4
EMODIF,ALL,MAT,2,

vsel,r,volu, ,10,12,1
nslv,r,1
allsel,below,volu
nset,r,loc,z,0

cm,ad1,nodes
alls,all
nsle
eplot
vsel,r,volu, ,10,12,1
nslv,r,1
allsel,below,volu
nset,r,loc,z,ta
cm,ad2,nodes
allsel,all
nplot
alls,all
eplot
alls,all

!patch modeling!!!!!!!!!!!!!!!!!!!!!!!!!!!!

k,59,(0.5*PW-G),(PL/2),ta

```

k,60,-(0.5\*PW-G),(PL/2),ta  
k,61,-PW/2,(0.5\*PL-G),ta  
k,62,PW/2,(0.5\*PL-G),ta  
k,63,-PW/2,-(0.5\*PL-G),ta  
k,64,(0.5\*PW-G),-(PL/2),ta  
k,65,-(0.5\*PW-G),-(PL/2),ta  
k,66,PW/2,-(0.5\*PL-G),ta

k,67,PW/2-G,-(0.5\*PL-3.9),ta  
k,68,-(PW/2-G),-(0.5\*PL-3.9),ta  
k,69,PW/2,-(0.5\*PL-G-3.9),ta  
k,70,-(PW/2),-(0.5\*PL-G-3.9),ta

k,71,PW/2-G,(0.5\*PL-3.9),ta  
k,72,-(PW/2-G),(0.5\*PL-3.9),ta  
k,73,PW/2,(0.5\*PL-G-3.9),ta  
k,74,-(PW/2),(0.5\*PL-G-3.9),ta

a,74,61,60,72  
a,60,59,71,72  
a,59,71,73,62  
a,74,72,71,73  
a,74,70,69,73  
a,70,63,65,68  
a,68,67,69,70  
a,68,65,64,67  
a,67,64,66,69

aplot

asel,r,area,,59,68,1  
VEXT,all,,0,0,tp,,,,  
a,59,62,47,46  
a,59,46,44,60  
a,60,44,41,61  
a,64,78,50,66  
a,64,78,77,65  
a,63,49,77,65  
VSBA, 14, 102  
VSBA, 15, 101  
VSBA, 13, 103  
VSBA, 21, 104  
VSBA, 20, 105  
VSBA, 18, 106

```

vdele,23,28,,1
/rep
vsel,r,volu,,13,15,1
ASLV
lsla
lplot
lsel,u,loc,z,ta
lsel,u,loc,z,tp
LESIZE,all,,6,,0
alls,all
vsel,u,volu,,10,12,1
vsel,u,volu,,1,9,1
vsel,r,volu,,13,22,1
ASLV
LESIZE,ALL,,-1,1
lplot
ASLV
lsla
lplot

lsel,r,loc,y,p1/2
lsel,a,loc,y,-p1/2
LESIZE,all,,10,,0
alls,all
vsel,r,volu,,13,22,1
ASLV
vsel,u,volu,,18
ASLV
lsla
lplot
LESIZE,ALL,,-1,1
lsel,r,loc,x,pw/2-g,pw/2

lsel,u,loc,x,pw/2
LESIZE,all,,5,,0
alls,all
vsel,r,volu,,13,22,1
ASLV
vsel,u,volu,,18
ASLV
lsla
lplot
LESIZE,ALL,,-1,1

```

```

lselect,a,loc,x,-(pw/2-g),-pw/2
lselect,u,loc,x,-pw/2
LESIZE,all,,5,,,,,0
alls,all
vselect,r,volu,,13,22,1
ASLV
vselect,u,volu,,18
ASLV
LESIZE,ALL,,,-1,,1
lplot
lsla
lplot
lselect,r,loc,x,pw/2
lselect,a,loc,x,-pw/2
LESIZE,all,,20,,,,,0
alls,all
vselect,r,volu,,13,22,1
ASLV
vselect,u,volu,,18
ASLV
LESIZE,ALL,,,-1,,1
lplot
lsla
lplot
lselect,r,loc,y,pl/2-G
lselect,a,loc,y,-(pL/2-G)
LESIZE,all,,10,,,,,0
alls,all
ALLS,ALL

ALLS,ALL
vselect,r,volu,,13,22,1
ASLV
vselect,u,volu,,18
ASLV
vsweep,all
cselect,u,panel,elem
cselect,u,adhesive,elem
cm,patch,elem
uimp,3,ex,ey,ez,81900,6150,6150
uimp,3,gxy,gyz,gxz,2770,2050,2770
uimp,3,prxy,pryz,prxz,0.34,0.5,0.34
EMODIF,ALL,MAT,3,

```

```

alls,all
eplot
ALLS,ALL
vsel,r,volu,,13,22,1
ASLV
vsel,u,volu,,18
ASLV
nslv,r,1
nset,r,loc,z,ta
cm,pd1,nodes
allsel,all
nsle
eplot
ALLS,ALL
vsel,r,volu,,13,22,1
ASLV
vsel,u,volu,,18
ASLV
eslv,r,1

cmsel,s,patch
nsle
eplot
local,11,0,0,0,0,90
emodif,all,esys,11
esys,0
csys,0
alls,all
nsle
eplot

!!!!!!!!!!!!!!bottom adhesive modeling!!!!!!!!!!!!!!

allsel,all
vsel,r,volu,,10,12,1
allsel,below,volu
nslv,r,1

vgen,2,all,,,,-(ts+ta),,,
vsel,u,volu,,10,12
nslv,r,1
allsel,below,volu

```

```

mp,ex,4,1148
mp,nuxy,4,0.4
EMODIF,ALL,MAT,4,
cm,adhesive1,elem
nselect,r,loc,z,-ts
cm,ad3,nodes
alls,all
cmsel,r,adhesive1
vsel,u,volu,,1,17
vsel,u,volu,,20,22
allsel,below,volu
nslv,r,1
epplot

nselect,r,loc,z,-(ts+ta)
nplot
cm,ad4,nodes
alls,all
epplot

!!!!!!!!!!bottom patch modeling2!!!!!!!!!!!!!!!!!!!!!!!!!!!!!!!!!!!!1

ALLS,ALL
vsel,r,volu,,13,22,1
ASLV
vsel,u,volu,,18
ASLV
nslv,r,1
vsymm,z,all,,,0,0
vsel,u,volu,,13,22,1

cmsel,u,patch,elem
allsel,below,volu

VGEN,,all,,,-(ts),,,1
vsel,r,volu,,25,33,1
allsel,below,volu
uimp,5,ex,ey,ez,81900,6150,6150
uimp,5,gxy,gyz,gxz,2770,2050,2770
uimp,5,prxy,pryz,prxz,0.34,0.5,0.34
EMODIF,ALL,MAT,5,
cm,patch1,elem
ALLS,ALL

```



```

vsel,r,volu,,25,33,1
allsel,below,volu
ASLV
eslv,r,1
nslv,r,1
nsel,r,loc,z,-(ts+ta)
cm,pd2,nodes
allsel,all
nsle
eplot
cmsel,r,panel
nsle
eplot
mp,ex,1,73100
mp,nuxy,1,0.3
emodif,all,mat,1

!!!!!!!!!!!!!!!!!!!!!!!!!!!!MPC CONTACT ALGORITHM!!!!!!!!!!!!!!!!!!!!
alls,all
eplot
/COM, CONTACT PAIR CREATION - START
CM,_NODECM,NODE
CM,_ELEMCM,ELEM
CM,_KPCM,KP
CM,_LINECM,LINE
CM,_AREACM,AREA
CM,_VOLUCM,VOLU
/GSAV,cwz,gsav,,temp
MP,MU,1,
MAT,6
MP,EMIS,2,7.88860905221e-31
R,3
REAL,3
ET,2,170
ET,3,174
R,3,,,-114,0.1,0,
RMORE,, ,1.0E20,0.0,1.0,-114
RMORE,0.0,0,1.0,,1.0,0.5
RMORE,0,1.0,1.0,0.0,,1.0
KEYOPT,3,4,0
KEYOPT,3,5,0
KEYOPT,3,7,0
KEYOPT,3,8,0

```

```

KEYOPT,3,9,0
KEYOPT,3,10,2
KEYOPT,3,11,0
KEYOPT,3,12,5
KEYOPT,3,2,0
KEYOPT,2,5,0
! Generate the target surface
NSEL,S,,P1
CM,_TARGET,NODE
TYPE,2
ESLN,S,0
ESURF
CMSEL,S,_ELEMCM
! Generate the contact surface
NSEL,S,,AD1
CM,_CONTACT,NODE
TYPE,3
ESLN,S,0
ESURF
ALLSEL
ESEL,ALL
ESEL,S,TYPE,,2
ESEL,A,TYPE,,3
ESEL,R,REAL,,3
/PSYMB,ESYS,1
/PNUM,TYPE,1
/NUM,1
EPLLOT
ESEL,ALL
ESEL,S,TYPE,,2
ESEL,A,TYPE,,3
ESEL,R,REAL,,3
CMSEL,A,_NODECM
CMDEL,_NODECM
CMSEL,A,_ELEMCM
CMDEL,_ELEMCM
CMSEL,S,_KPCM
CMDEL,_KPCM
CMSEL,S,_LINECM
CMDEL,_LINECM
CMSEL,S,_AREACM
CMDEL,_AREACM
CMSEL,S,_VOLUCM

```

```

CMDEL,_VOLUCM
/GRES,cwz,gsav
CMDEL,_TARGET
CMDEL,_CONTACT
/COM, CONTACT PAIR CREATION - END
/COM, CONTACT PAIR CREATION - START
CM,_NODECM,NODE
CM,_ELEMCM,ELEM
CM,_KPCM,KP
CM,_LINECM,LINE
CM,_AREACM,AREA
CM,_VOLUCM,VOLU
/GSAV,cwz,gsav,,temp
MP,MU,1,0
MAT,6
MP,EMIS,2,7.88860905221e-31
R,4
REAL,4
ET,4,170
ET,5,174
R,4,,,-114,0.1,0,
RMORE,,1.0E20,0.0,1.0,-114
RMORE,0.0,0,1.0,,1.0,0.5
RMORE,0,1.0,1.0,0.0,,1.0
KEYOPT,5,4,0
KEYOPT,5,5,0
KEYOPT,5,7,0
KEYOPT,5,8,0
KEYOPT,5,9,0
KEYOPT,5,10,2
KEYOPT,5,11,0
KEYOPT,5,12,5
KEYOPT,5,2,0
KEYOPT,4,5,0
! Generate the target surface
NSEL,S,,AD2
CM,_TARGET,NODE
TYPE,4
ESLN,S,0
ESURF
CMSEL,S,_ELEMCM
! Generate the contact surface
NSEL,S,,PD1

```

```

CM, _CONTACT, NODE
TYPE, 5
ESLN, S, 0
ESURF
ALLSEL
ESEL, ALL
ESEL, S, TYPE, , 4
ESEL, A, TYPE, , 5
ESEL, R, REAL, , 4
/PSYMB, ESYS, 1
/PNUM, TYPE, 1
/NUM, 1
EPLLOT
ESEL, ALL
ESEL, S, TYPE, , 4
ESEL, A, TYPE, , 5
ESEL, R, REAL, , 4
CMSEL, A, _NODECM
CMDEL, _NODECM
CMSEL, A, _ELEMCM
CMDEL, _ELEMCM
CMSEL, S, _KPCM
CMDEL, _KPCM
CMSEL, S, _LINECM
CMDEL, _LINECM
CMSEL, S, _AREACM
CMDEL, _AREACM
CMSEL, S, _VOLUCM
CMDEL, _VOLUCM
/GRES, cwz, gsav
CMDEL, _TARGET
CMDEL, _CONTACT
/COM, CONTACT PAIR CREATION - END
/COM, CONTACT PAIR CREATION - START
CM, _NODECM, NODE
CM, _ELEMCM, ELEM
CM, _KPCM, KP
CM, _LINECM, LINE
CM, _AREACM, AREA
CM, _VOLUCM, VOLU
/GSAV, cwz, gsav, , temp
MP, MU, 1, 0
MAT, 6

```

```

MP,EMIS,2,7.88860905221e-31
R,5
REAL,5
ET,6,170
ET,7,174
R,5,,,-114,0.1,0,
RMORE,,1.0E20,0.0,1.0,-114
RMORE,0.0,0,1.0,,1.0,0.5
RMORE,0,1.0,1.0,0.0,,1.0
KEYOPT,7,4,0
KEYOPT,7,5,0
KEYOPT,7,7,0
KEYOPT,7,8,0
KEYOPT,7,9,0
KEYOPT,7,10,2
KEYOPT,7,11,0
KEYOPT,7,12,5
KEYOPT,7,2,0
KEYOPT,6,5,0
! Generate the target surface
NSEL,S,,P2
CM,_TARGET,NODE
TYPE,6
ESLN,S,0
ESURF
CMSEL,S,_ELEMCM
! Generate the contact surface
NSEL,S,,AD3
CM,_CONTACT,NODE
TYPE,7
ESLN,S,0
ESURF
ALLSEL
ESEL,ALL
ESEL,S,TYPE,,6
ESEL,A,TYPE,,7
ESEL,R,REAL,,5
/PSYMB,ESYS,1
/PNUM,TYPE,1
/NUM,1
EPLLOT
ESEL,ALL
ESEL,S,TYPE,,6

```

```

ESEL,A,TYPE,,7
ESEL,R,REAL,,5
CMSEL,A,_NODECM
CMDEL,_NODECM
CMSEL,A,_ELEMCM
CMDEL,_ELEMCM
CMSEL,S,_KPCM
CMDEL,_KPCM
CMSEL,S,_LINECM
CMDEL,_LINECM
CMSEL,S,_AREACM
CMDEL,_AREACM
CMSEL,S,_VOLUCM
CMDEL,_VOLUCM
/GRES,cwz,gsav
CMDEL,_TARGET
CMDEL,_CONTACT
/COM, CONTACT PAIR CREATION - END
/COM, CONTACT PAIR CREATION - START
CM,_NODECM,NODE
CM,_ELEMCM,ELEM
CM,_KPCM,KP
CM,_LINECM,LINE
CM,_AREACM,AREA
CM,_VOLUCM,VOLU
/GSAV,cwz,gsav,,temp
MP,MU,1,0
MAT,6
MP,EMIS,2,7.88860905221e-31
R,6
REAL,6
ET,8,170
ET,9,174
R,6,,, -114,0.1,0,
RMORE,,,1.0E20,0.0,1.0, -114
RMORE,0.0,0,1.0,,1.0,0.5
RMORE,0,1.0,1.0,0.0,,1.0
KEYOPT,9,4,0
KEYOPT,9,5,0
KEYOPT,9,7,0
KEYOPT,9,8,0
KEYOPT,9,9,0
KEYOPT,9,10,2

```

```

KEYOPT,9,11,0
KEYOPT,9,12,5
KEYOPT,9,2,0
KEYOPT,8,5,0
! Generate the target surface
NSEL,S,,AD4
CM,_TARGET,NODE
TYPE,8
ESLN,S,0
ESURF
CMSEL,S,_ELEMCM
! Generate the contact surface
NSEL,S,,PD2
CM,_CONTACT,NODE
TYPE,9
ESLN,S,0
ESURF
ALLSEL
ESEL,ALL
ESEL,S,TYPE,,8
ESEL,A,TYPE,,9
ESEL,R,REAL,,6
/PSYMB,ESYS,1
/PNUM,TYPE,1
/NUM,1
EPLLOT
ESEL,ALL
ESEL,S,TYPE,,8
ESEL,A,TYPE,,9
ESEL,R,REAL,,6
CMSEL,A,_NODECM
CMDEL,_NODECM
CMSEL,A,_ELEMCM
CMDEL,_ELEMCM
CMSEL,S,_KPCM
CMDEL,_KPCM
CMSEL,S,_LINECM
CMDEL,_LINECM
CMSEL,S,_AREACM
CMDEL,_AREACM
CMSEL,S,_VOLUCM
CMDEL,_VOLUCM
/GRES,cwz,gsav

```

```

CMDEL,_TARGET
CMDEL,_CONTACT
/COM, CONTACT PAIR CREATION - END
/MREP,EPLOTT
alls,all
eploTT
nseL,r,loc,y,-80
D,ALL, ,0, , , ,ALL, , , , ,
ALLS,ALL
NSEL,R,LOC,Y,80
SF,ALL,PRES,-250
alls,all

esel,s,adj,,2789
esel,a,adj,,6749
nsle
eploTT
emodif,all,mat,2
/rep
alls,all
nsle
eploTT

esel,s,adj,,5293
esel,a,adj,,7768
nsle
eploTT
emodif,all,mat,3
emodif,all,esys,11

alls,all
esel,s,adj,,1793
nsle
eploTT
cm,panel,elems
nsle
eploTT
emodif,all,mat,1
alls,all
nsle
eploTT
FINISH
/SOLU

```



SOLVE  
FINISH  
/EXIT,SOLU

# References

- [1] [https://en.wikipedia.org/wiki/File:F-89\\_Scorpion\\_Crash\\_IAE\\_Detroit\\_1952.jpg](https://en.wikipedia.org/wiki/File:F-89_Scorpion_Crash_IAE_Detroit_1952.jpg).
- [2] [https://en.wikipedia.org/wiki/File:DH\\_Comet\\_1\\_BOAC\\_Heathrow\\_1953.jpg](https://en.wikipedia.org/wiki/File:DH_Comet_1_BOAC_Heathrow_1953.jpg).
- [3] [https://en.wikipedia.org/wiki/File:Comet\\_1\\_G-ALYP\\_-\\_wreckage\\_recovered\\_png.png](https://en.wikipedia.org/wiki/File:Comet_1_G-ALYP_-_wreckage_recovered_png.png).
- [4] [https://en.wikipedia.org/wiki/File:Fuselage\\_of\\_de\\_Havilland\\_Comet\\_Airliner\\_G-ALYP.JPG](https://en.wikipedia.org/wiki/File:Fuselage_of_de_Havilland_Comet_Airliner_G-ALYP.JPG).
- [5] <http://www.interfaceforce.com/index.php?Full-Scale-Fatigue-Testing&mod=applications&show=23>.
- [6] M. Ramji and R. Srilakshmi. Design of composite patch reinforcement applied to mixed-mode cracked panel using finite element analysis. *Journal of Reinforced Plastics and Composites* 31, (2012) 585–595.
- [7] <http://www.adhesivestoolkit.com>.
- [8] [http://www.fea-optimization.com/ETBX/miner\\_help\\_files/figure2.gif](http://www.fea-optimization.com/ETBX/miner_help_files/figure2.gif).
- [9] [http://www.fea-optimization.com/ETBX/miner\\_help\\_files/figure1.gif](http://www.fea-optimization.com/ETBX/miner_help_files/figure1.gif).
- [10] <http://www.nlr.nl/>.
- [11] <http://www.zentech.co.uk/>.
- [12] <http://asm.matweb.com/search/SpecificMaterial.asp?bassnum=MA2014T6>.
- [13] M. Kashfuddoja and M. Ramji. Critical analysis of adhesive layer behavior in patch-repaired carbon fiber-reinforced polymer panel involving digital image correlation. *Journal of Composite Materials* 49, (2014) 2015–2028.
- [14] M. Kashfuddoja, R. Prasath, and M. Ramji. Study on experimental characterization of carbon fiber reinforced polymer panel using digital image correlation: A sensitivity analysis. *Optics and Lasers in Engineering* 62, (2014) 17–30.
- [15] R. Srilakshmi, M. Ramji, and V. Chinthapenta. Fatigue crack growth study of CFRP patch repaired Al 2014-T6 panel having an inclined center crack using FEA and DIC. *Engineering Fracture Mechanics* 134, (2015) 182–201.

- [16] <http://www3.gendisasters.com/michigan/18997/detroit-mi-air-show-accident-aug-1952>.
- [17] [https://en.wikipedia.org/wiki/BOAC\\_Flight\\_781](https://en.wikipedia.org/wiki/BOAC_Flight_781).
- [18] A. Baker. Chapter 1 - Introduction and Overview. In A. B. R. Jones, ed., *Advances in the Bonded Composite Repair of Metallic Aircraft Structure*, 1 – 18. Elsevier Science Ltd, Oxford, 2002.
- [19] J. Schijve. Four lectures on fatigue crack growth: I. Fatigue crack growth and fracture mechanics. *Engineering Fracture Mechanics* 11, (1979) 169 – 181.
- [20] R. Sunder. A mathematical model of fatigue crack propagation under variable amplitude loading. *Engineering Fracture Mechanics* 12.
- [21] J. Schijve. Crack growth in aluminium alloy sheet material under flight-simulation loading. *International Journal of Fatigue* 7.
- [22] R. Sunder. System for automated fatigue crack growth testing under random loading. *International Journal of Fatigue* 7, (1985) 3–12.
- [23] R. Sunder. Fatigue crack propagation under spectrum loading. *Journal of Aeronautical Society of India* 38, (1986) 153–160.
- [24] J. C. Newman, Jr. Prediction of Crack Growth Under Variable-Amplitude Loading in Various Materials. Technical Report 1997.
- [25] C. Manjunatha and V. Ranganath. Prediction of Optimum Spectrum for Full Scale Fatigue Test. In 15th National Seminar on Aerospace Structures. 2007 192–197.
- [26] C. Manjunatha, R. Bojja, N. Jagannathan, A. Kinloch, and A. Taylor. Enhanced fatigue behavior of a glass fiber reinforced hybrid particles modified epoxy nanocomposite under WISPERX spectrum load sequence. *International Journal of Fatigue* 54, (2013) 25–31.
- [27] H. Hosseini-Toudeshky, A. Jasemzadeh, and B. Mohammadi. Investigation of effective parameters on composite patch debonding under static and cyclic loading using cohesive elements. *Finite Elements in Analysis and Design* 74.
- [28] A. Maligno, C. Soutis, and V. Silberschmidt. An advanced numerical tool to study fatigue crack propagation in aluminium plates repaired with a composite patch. *Engineering Fracture Mechanics* 99.
- [29] [http://www.boeing.com/commercial/aeromagazine/articles/2012\\_q4/2/](http://www.boeing.com/commercial/aeromagazine/articles/2012_q4/2/).
- [30] D. Ouinas, B. B. Bouiadjra, S. Himouri, and N. Benderdouche. Progressive edge cracked aluminium plate repaired with adhesively bonded composite patch under full width disbond. *Composites Part B: Engineering* 43.
- [31] D. Ouinas, A. Hebbbar, B. B. Bouiadjra, M. Belhouari, and B. Serier. Numerical analysis of the stress intensity factors for repaired cracks from a notch with bonded composite semicircular patch. *Composites Part B: Engineering* 40.

- [32] P. Papanikos, K. Tserpes, and S. Pantelakis. Initiation and progression of composite patch debonding in adhesively repaired cracked metallic sheets. *Composite Structures* 81.
- [33] P. Papanikos, K. Tserpes, G. Labeas, and S. Pantelakis. Progressive damage modelling of bonded composite repairs. *Theoretical and Applied Fracture Mechanics* 43.
- [34] D.-C. Seo and J.-J. Lee. Fatigue crack growth behavior of cracked aluminum plate repaired with composite patch. *Composite Structures* 57, (2002) 323–330.
- [35] B. Ziegler, Y. Yamada, and J. Newman. Application of a strip-yield model to predict crack growth under variable-amplitude and spectrum loading – Part 2: Middle-crack-tension specimens. *Engineering Fracture Mechanics* 78.
- [36] B. Moreno, A. Martin, P. Lopez-Crespo, J. Zapatero, and J. Dominguez. On the Use of NASGRO Software to Estimate Fatigue Crack Growth under Variable Amplitude Loading in Aluminium Alloy 2024-T351. *Procedia Engineering* 101.
- [37] M. Ramji, R. Srilakshmi, and M. B. Prakash. Towards optimization of patch shape on the performance of bonded composite repair using FEM. *Composites Part B: Engineering* 45.
- [38] R. Srilakshmi and M. Ramji. Experimental investigation of adhesively bonded patch repair of an inclined center cracked panel using DIC. *Journal of Reinforced Plastics and Composites* 33, (2014) 1130–1147.
- [39] Test Method for Measurement of Fatigue Crack Growth Rates.
- [40] H. Toutanji, S. Ueno, and R. Vuddandam. Prediction of the interfacial shear stress of externally bonded FRP to concrete substrate using critical stress state criterion. *Composite Structures* 95, (2013) 375–380.